

ICES REPORT 10-17

May 2010

A Class of Discontinuous Petrov-Galerkin Methods. Part IV: Wave Propagation

by

J. Zitelli, I. Muga, L. Demkowicz, J. Gopalakrishnan, D. Pardo, and V. M. Calo



The Institute for Computational Engineering and Sciences
The University of Texas at Austin
Austin, Texas 78712

Reference: J. Zitelli, I. Muga, L. Demkowicz, J. Gopalakrishnan, D. Pardo, and V.M. Calo, "A Class of Discontinuous Petrov-Galerkin Methods. Part IV: Wave Propagation", ICES REPORT 10-17, The Institute for Computational Engineering and Sciences, The University of Texas at Austin, May 2010.

A CLASS OF DISCONTINUOUS PETROV-GALERKIN METHODS. PART IV: WAVE PROPAGATION

J. ZITELLI, I. MUGA, L. DEMKOWICZ, J. GOPALAKRISHNAN, D. PARDO, AND V. M. CALO

ABSTRACT. The phase error, or the pollution effect in the finite element solution of wave propagation problems, is a well known phenomenon that must be confronted when solving problems in the high-frequency range. This paper presents a new method with *no phase errors* for one-dimensional time-harmonic wave propagation problems. The method is constructed within the framework of the Discontinuous Petrov-Galerkin (DPG) method with optimal test functions. We have previously shown that such methods pick solutions that are the best possible approximations in an energy norm dual to any selected test space norm. In this paper, we advance by asking what is the *optimal test space norm* to achieve error reduction in a given energy norm. This is answered in the specific case of the Helmholtz equation with L^2 -norm as the energy norm. We obtain uniform stability with respect to the wave number k , thus eliminating the phase error of the numerical solution. We illustrate the method with a number of 1D numerical experiments, using discontinuous (L^2 -conforming) piecewise polynomials hp spaces for the trial space with the corresponding optimal test functions computed approximately at the element level. The 1D experiments are accompanied with a complete stability analysis.

1. INTRODUCTION

The aim of this paper is to introduce a new methodology to design schemes for wave-propagation problems. It is a continuation of our research on Discontinuous Petrov-Galerkin (DPG) methods [9, 10, 11]. Our previous papers applied the DPG methodology to get new methods for convective and diffusive phenomena. In this paper, we apply it to wave propagation after developing additionally needed theoretical tools.

The numerical solution of wave propagation problems at high frequencies has been recognized as an outstanding challenge in numerical analysis. In general, numerical methods for wave propagation are subject to the effect of *pollution*: increasing the frequency, while maintaining the approximation quality of the numerical discretization, results in a divergence of the computed result from the best approximation provided by the discretization, which grows unboundedly as the frequency is increased. In the context of finite element methods, the pollution error may be characterized as follows [23]: given an approximation space $U_h \subset U$ with a corresponding norm in which we measure the error of the exact solution $u \in U$, the approximation u_h satisfies

$$\frac{\|u - u_h\|_U}{\|u\|_U} \leq C(k) \inf_{w_h \in U_h} \frac{\|u - w_h\|_U}{\|u\|_U},$$

where

$$C(k) = C_1 + C_2 k^\beta (kh)^\gamma,$$

2000 *Mathematics Subject Classification.* 65N30, 35L15.

Key words and phrases. time harmonic, wave propagation, Helmholtz, DPG, Discontinuous Petrov Galerkin, robustness, phase error, dispersion.

J. Zitelli was supported by an ONR Graduate Traineeship and CAM Fellowship. I. Muga was supported by Sistema Bicentenario BECAS CHILE (Chilean Government). L. Demkowicz was supported by a Collaborative Research Grant from King Abdullah University of Science and Technology (KAUST). J. Gopalakrishnan was supported by the National Science Foundation under grant DMS-0713833.

with k being the wavenumber, and h being the element size. The k -dependence of the stability constant C reflects the growing instability of the problem at the continuous level, i.e. the inf-sup constant decreases as k increases. Generally, the exponent β is found to be one [23, 25], i.e. the pollution term in the error increases linearly with frequency. For many model problems, the pollution is manifested as a phase error which accumulates over the domain, and the concepts of pollution, phase error, and discrete wavenumbers are therefore all closely related. The growth of the pollution error, combined with the already difficult problem of approximating the highly oscillatory solutions of wave problems, can render numerical solution extremely expensive for high wavenumbers.

The main result of our application of the DPG methodology to one-dimensional wave propagation is a Petrov-Galerkin method which is free of pollution, i.e. $\beta = 0$. A number of previous methods have also achieved this goal in 1D, while reducing the severity of the pollution error in higher dimensions. One can find surveys of such methods in, e.g., [27, 19]. Broadly, they may be classified as follows: Galerkin/Least-Squares based methods ([20, 28]), which achieve improved stability by adding least squares residual terms to the standard Galerkin sesquilinear form; methods utilizing specialized, under-integrating quadrature rules ([1]) which reduce the phase error, as indicated by dispersion analysis of an interior stencil; and methods incorporating exact solutions of the Helmholtz equation (in particular, plane waves) within the trial space basis ([14, 15, 16, 3]).

Petrov-Galerkin formulations also appear frequently in the construction of stabilized methods (see, e.g. [22, 12, 13].) Common to such methods is the introduction of local problems which are solved to provide a trial/test space pair which provides enhanced stability. A few of these methods have attempted to address in particular the Helmholtz equation.

In the nearly optimal Petrov-Galerkin method (NOPG) of Barbone and Harari [5], the authors construct a method with the goal of achieving the best approximation in the H^1 seminorm in a given trial space. They show that the corresponding minimization problem leads to a Petrov-Galerkin formulation with optimal test functions with global support; by considering only local test functions constructed by adding bubbles to the standard basis functions, they arrive at a more practical formulation which approximates the H^1 -optimal result. For rectangular/hexahedral elements, the bubble functions may be determined analytically; more generally, the bubbles may be approximated numerically through local Galerkin problems. In certain cases, the method is equivalent to that of residual-free bubbles [17].

The quasi-optimal Petrov-Galerkin (QOPG) method of Loula and Fernandes [24] considers test functions constructed from a linear combination of standard bilinear Lagrangian basis functions and additional bubbles which are products of the same basis functions. The test functions are determined by solving locally a least-squares problem attempting to minimize a residual corresponding to the Lagrange interpolant of plane waves of all directions. For a uniform mesh, the phase error determined by analysis of an interior stencil is of the same order as that of the Quasi-Stabilized FEM (QSFEM) of Babuska et al. [2], i.e.

$$\frac{|k - k_h|}{k} \leq 1.5 \left(\frac{(kh)^6}{774144} \right).$$

The method we present for Helmholtz problems is very similar in spirit to these other approaches, i.e. it attempts to achieve optimal results in some sense by local computation of corresponding optimal test functions. The use of the DPG setting introduced by Bottaso, Micheletti, Sacco and Causin is where we depart; rather than starting from a traditional H^1 variational formulation in terms of pressure, the DPG setting introduces a mixed formulation for both pressure and velocity, which are now in L^2 , as well as additional fluxes. The goal which guides us in the definition of the test functions is to achieve the best approximation in the L^2 norm for both pressure and velocity.

The crucial property of the DPG methodology is that it guarantees the *best approximation property* in the so-called energy (dual, residual) norm. This norm is problem-dependent - it is implied by the operator governing the problem *and the choice of norm for the test space*. In our study on convection-dominated diffusion problems presented in [10, 11], our choices of norms for the test spaces consisted of standard Sobolev norms modified with additional weights to ensure robustness of the resulting method with respect to diffusion and introduced mesh-dependent factors to counter-fight round-off errors. In this report, we take a different approach and introduce a problem-dependent *optimal test norm*, constructed specifically to induce the desired energy norm, e.g. the L^2 norm for the problems we consider. Employing the exact optimal test functions corresponding to this test norm therefore yields a method which achieves the best approximation error in the L^2 norm; however, these test functions have global support, and find ourselves in a situation much like that pointed out in [18], i.e. although evaluation of the left hand side matrix is straightforward (by construction, it corresponds to the L^2 inner product), the work has been moved to determining the global optimal test functions which are needed to define the load vector. The approach then taken is to design a closely related and equivalent test norm which possesses local optimal test functions, which may be approximated through local Galerkin problems. This new test norm is equivalent to the optimal one *uniformly in wavenumber k* , and consequently so are the corresponding energy norms.

The report is structured as follows. First we introduce an abstract framework for the method (Section 2), related to the notions of *optimal test norm*, equivalent norms and the DPG method implementability. Next we apply the framework to two time-harmonic wave propagation problems, starting with a simple convection-reaction equation (Section 3) and continuing with the Helmholtz equation in a first-order setting (Section 4). Both problems are illustrated with extensive numerical examples. For the Helmholtz equation case, we additionally combine our method with a PML truncation. Conclusions are presented in Section 5. Appendix 1 discusses the *localization principle* which allows us to analyze DPG formulations *globally*, and Appendix 2 contains some technical details on the equivalence relations between norms.

2. PETROV-GALERKIN METHOD WITH OPTIMAL TEST NORM

The new methodology for constructing schemes is introduced in this section. Here we recall the DPG framework [9, 10] and the concept of optimal test functions introduced in [10]. This is presented together with the new concept of optimal test norm. In later sections we apply these abstract results to specific wave propagation examples.

2.1. Abstract setting. Consider an arbitrary abstract variational problem,

$$\begin{cases} \text{Find } u \in U \text{ such that :} \\ b(u, v) = l(v), \quad \forall v \in V. \end{cases} \quad (2.1)$$

Here U, V are two reflexive Banach spaces over \mathbb{C} (the complex field), $b(u, v)$ is a continuous sesquilinear form on $U \times V$ and $l(v)$ is a continuous conjugate linear form on V representing the load. (This terminology is standard – see [29]. Conjugate linear forms have also been called antilinear forms [26].)

We denote by U' the space of continuous linear functionals on U and by V^* the space of continuous conjugate linear functionals on V . The sesquilinear form b generates two continuous operators, B and B' , defined by

$$\begin{aligned} B : U &\rightarrow V^* \quad \text{such that} \quad Bu(v) = b(u, v), \quad \forall u \in U, \forall v \in V, \\ B' : V &\rightarrow U' \quad \text{such that} \quad B'v(u) = b(u, v), \quad \forall u \in U, \forall v \in V. \end{aligned}$$

The conjugate operator of a linear operator $L : E \rightarrow F$ is $L^* : F' \rightarrow E'$, defined by $L^*f(e) = f(Le)$ for all $f \in F'$ and $e \in E$. Since V is reflexive, there is an invertible (conjugate linear)

isometry $I_V : V \rightarrow (V^*)'$ such that $I_V v(v^*) = v^*(v)$ for all $v \in V$ and $v^* \in V^*$. It is easy to check that

$$B^* \circ I_V = B'. \quad (2.2)$$

We assume now that the operator B is invertible with continuous inverse $B^{-1} : V^* \rightarrow U$. We also assume that the operator B' is injective, which implies that it also has a continuous inverse (see e.g. [8, 26]). Then the problem (2.1) is clearly well-posed. Moreover, since $(B^*)^{-1} = (B^{-1})^*$, it follows from (2.2) that

$$(B')^{-1} = I_V^{-1} \circ (B^{-1})^*. \quad (2.3)$$

2.2. The optimal test space norm. We now restrict ourselves to the case where the “trial space” U is a Hilbert space with an inner product $(\cdot, \cdot)_U$ and corresponding norm $\|\cdot\|_U$. We define the *optimal test norm* on the “test space” V by

$$\|v\|_V := \sup_{u \in U} \frac{|b(u, v)|}{\|u\|_U}. \quad (2.4)$$

Since B' is a bijection, this norm generates a topology equivalent to the original topology in V (so we will have no use for the original norm on V). It is easy to see that the optimal test norm is generated by the inner product

$$(w, v)_V := b(R_U^{-1} B' w, v)$$

where $R_U : U \rightarrow U'$ is the isometric Riesz operator defined by $R_U u(v) = (v, u)_U$ for all $u \in U$ and $v \in V$. Thus, we have made V into a Hilbert space.

2.3. The optimal test functions. Now we recall the *Petrov-Galerkin scheme* of [10]. In [10], the method was presented using a general inner product on V . In contrast, here we are interested in using the specific inner product $(\cdot, \cdot)_V$ with its corresponding optimal test norm $\|\cdot\|_V$ introduced above.

Let $U_N \subset U$ be a finite-dimensional space with a basis $\{e_j : j = 1, \dots, N\}$. Define $T : U \rightarrow V$ by

$$(Tu, v)_V = b(u, v), \quad \forall v \in V. \quad (2.5)$$

For each *trial* basis function e_j , the corresponding *optimal test (basis) function* is $Te_j \in V$. They form optimal discrete test space

$$V_N := \text{span}\{Te_j : j = 1, \dots, N\} \subset V. \quad (2.6)$$

The *Petrov-Galerkin scheme* for (2.1) is as follows.

$$\begin{cases} \text{Find } u_N \in U_N \text{ such that :} \\ b(u_N, v_N) = l(v_N), \quad \forall v_N \in V_N. \end{cases} \quad (2.7)$$

This can be thought of as a least square method [6] as explained in [10]. It is proven in [10, Theorem 2.2] (and the proof is simple) that in the *energy norm* defined by

$$\|u\|_E := \sup_{v \in V} \frac{|b(u, v)|}{\|v\|_V}, \quad (2.8)$$

the solution of the *Petrov-Galerkin scheme* (2.7) is the best approximation, i.e.,

$$\|u - u_N\|_E = \inf_{w_N \in U_N} \|u - w_N\|_E. \quad (2.9)$$

While it is difficult to characterize $\|\cdot\|_E$ in general [10], because we used the optimal test norm $\|\cdot\|_V$ of § 2.2 in (2.8), we have the following simple characterization.

Proposition 2.1. *For all $u \in U$, we have $\|u\|_E = \|u\|_U$, and consequently,*

$$\|u - u_N\|_U = \inf_{w_N \in U_N} \|u - w_N\|_U. \quad (2.10)$$

Proof. By (2.4), $|b(u, v)| \leq \|u\|_U \|v\|_V$, so obviously $\|u\|_E \leq \|u\|_U$. The reverse inequality obviously follows if we prove that

$$\inf_{u \in U} \frac{\|u\|_E}{\|u\|_U} = \inf_{u \in U} \sup_{v \in V} \frac{|b(u, v)|}{\|u\|_U \|v\|_V} = \inf_{v \in V} \sup_{u \in U} \frac{|b(u, v)|}{\|v\|_V \|u\|_U} = 1. \quad (2.11)$$

The last equality in (2.11) is obvious from (2.4). The first inf-sup equals $1/\|B^{-1}\|$, while the second equals $1/\|(B')^{-1}\|$ (where $\|\cdot\|$ denotes the appropriate operator norms). They are equal by (2.3). Hence (2.11) follows and we have proved that $\|u\|_E = \|u\|_U$. Using this, (2.10) follows from (2.9). \square

We note two properties of the *Petrov-Galerkin scheme* (2.7).

- (1) The global stiffness matrix of the method is *Hermitian and positive definite* irrespective of the symmetry properties of $b(\cdot, \cdot)$. Indeed,

$$b(e_i, Te_j) = (Te_i, Te_j)_V = \overline{(Te_j, Te_i)}_V = \overline{b(e_j, Te_i)},$$

so it is Hermitian. Positive definiteness follows from (2.5). This property is a manifestation of the least square nature of the method.

- (2) Once the approximate solution has been determined, the norm of the finite element error $e_N := u - u_N$ can be computed once we solve the following problem:

$$\begin{cases} \text{Find } Te_N \in V \text{ such that :} \\ (Te_N, \delta v)_V = b(u - u_N, \delta v) = l(\delta v) - b(u_N, \delta v), \quad \forall \delta v \in V. \end{cases} \quad (2.12)$$

Then,

$$\|e_N\|_U = \|e_N\|_E = \|Te_N\|_V. \quad (2.13)$$

We call the solution Te_N to problem (2.12) *the error representation function*. Notice that we can compute a good approximation to energy norm of the error *without knowing* the exact solution by solving an approximate version of (2.12). Indeed, the energy norm of the error is nothing other than a properly defined norm of the residual.

2.4. Equivalent test norms. In our examples later, the optimal norm $\|\cdot\|_V$ turns out to be inconvenient for practical computations. Hence we investigate changes that result when it is substituted with another norm $\|\cdot\|_{\tilde{V}}$ satisfying

$$C_1 \|v\|_{\tilde{V}} \leq \|v\|_V \leq C_2 \|v\|_{\tilde{V}}, \quad \forall v \in V. \quad (2.14)$$

We assume that the new norm is generated by an inner product $(\cdot, \cdot)_{\tilde{V}}$. When this is used in place of $(\cdot, \cdot)_V$ in (2.5), different optimal test functions, and consequently a different *Petrov-Galerkin scheme* results. Let us denote its solution by \tilde{u}_N . It is the best approximation in the following energy norm

$$\|u\|_{\tilde{E}} := \sup_{v \in V} \frac{|b(u, v)|}{\|v\|_{\tilde{V}}} \quad (2.15)$$

which in general is not equal to $\|u\|_U$. Yet, we have the following theorem.

Theorem 2.1. *Let C_1 and C_2 be the constants of the equivalence relation (2.16). Then*

$$\|u - \tilde{u}_N\|_U \leq \frac{C_2}{C_1} \inf_{w_N \in U_N} \|u - w_N\|_U.$$

Proof. The solution \tilde{u}_N (due to the result of [10] recalled in 2.9) satisfies

$$\|u - \tilde{u}_N\|_{\tilde{E}} = \inf_{w_N \in U_N} \|u - w_N\|_{\tilde{E}}.$$

Hence the theorem will follow if we show that

$$C_1 \|u\|_U \leq \|u\|_{\tilde{E}} \leq C_2 \|u\|_U, \quad \forall u \in U. \quad (2.16)$$

For any nonzero v in V , taking reciprocals in (2.14) we obtain

$$\frac{1}{C_2\|v\|_{\tilde{V}}} \leq \frac{1}{\|v\|_V} \leq \frac{1}{C_1\|v\|_{\tilde{V}}}. \quad (2.17)$$

Hence (2.16) follows by multiplying the inequality (2.17) by $|b(u, v)|$ and taking the supremum over all non-zero vectors $v \in V$. \square

From Theorem 2.1, it is clear that in order to achieve the good stability in $\|\cdot\|_U$, independent of problem parameters (e.g. wavenumber k in the problems we shall consider in the next sections), the alternative norm $\|\cdot\|_{\tilde{V}}$ should be designed so that the ratio of the equivalence factors, C_2/C_1 , is (i) as small as possible, and (ii) independent of the parameters.

2.5. Practicalities. For conforming discretizations, the application of T , which requires the solution of (2.5), leads to a global system of equations. Then the computation of optimal test space is too expensive and the entire discussed concept has little practical value.

The situation changes if the methodology is applied in the framework of *discontinuous* Petrov-Galerkin (DPG) method. When functions in V are discontinuous across mesh elements, and when the V -inner product is locally computable, then the solution of (2.5) becomes a local operation. By approximating these local problems suitably, test functions close to optimality can be inexpensively computed. In the methods we present, we use richer polynomial spaces (a few degrees higher than the trial spaces) to approximate (2.5).

To ensure that functions in V are discontinuous, we treat all equations of a boundary value problem weakly. The starting point in the design of a DPG method is a reformulation of the boundary value problem into a system of first-order differential equations. Introducing a partitioning of the spatial domain Ω into mesh elements $\{K\}$, the equations are multiplied element-wise by test functions in a “broken” test space

$$V = V_{\text{DPG}} = \prod_K V(K), \quad (2.18)$$

integrated over the whole domain, and then integrated by parts in each element. The resulting boundary flux terms are treated rather as *independent unknowns*. Fluxes known from boundary conditions are replaced or moved to the right-hand side where appropriate, contributing in that manner to the linear functional $l(v)$. Contrary to classical variational formulations where some of the equations are relaxed and others are treated in a strong form, in the DPG method *all equations* are treated in a weak sense. Formulations like this are sometimes referred to as *ultra-weak variational formulations*.

When using a general inner product on V , we can choose it to be local (as we did in [10, 11]). Unfortunately, the optimal V -inner product of the optimal test norm is generally not local because of the introduction of fluxes in the DPG formulation. In this situation, we must find an equivalent *localizable* \tilde{V} -inner product, i.e., its associated *localizable* \tilde{V} -norm satisfies

$$\|v\|_{\tilde{V}}^2 = \sum_K \|v_K\|_{\tilde{V}}^2, \quad \forall v \in V, \quad (2.19)$$

where v_K denotes the restriction of v to K , extended by zero to Ω . This maintains the locality of test space computations. Changes in the solution due to the substitution of the new inner product can be analyzed using the results in § 2.4.

For adaptivity, we can use the error indicator shown in (2.13). Its square equals the sum of corresponding element contributions, i.e.,

$$\|e_N\|_E^2 = \|Te_N\|_{V_{\text{DPG}}}^2 = \sum_K e_K, \quad (2.20)$$

where $e_K = \|(Te_N)_K\|_V^2$. The error representation function $(Te_N)_K$ on K is computed by solving a local counterpart of (2.12) using an element enriched space. The element contributions e_K serve as element error indicators in an hp -adaptive algorithm (see [11]).

3. A MODEL TIME-HARMONIC TRANSPORT PROBLEM

As a prelude to the DPG formulation of the full Helmholtz equation presented in Section 4, in this section we study a simplified 1D time-harmonic wave propagation problem. We begin by considering the *spectral* method, in which we use a globally-conforming test space V , and identify the explicit forms of the optimal test norm and inner product. We then consider the *DPG* method, utilizing a “broken” test space V_{DPG} . After identifying the optimal test norm and inner product in this setting, we present an equivalent *localizable* norm which may be practically utilized in the *DPG* setting. We then discuss the approximation of the optimal test functions in the numerical implementation, and present results demonstrating the stated robustness in both the spectral and DPG settings.

We consider the problem:

$$\begin{cases} ik\rho + \rho' = 0 & \text{in } (0, 1), \\ \rho(0) = \rho_0. \end{cases} \quad (3.21)$$

This arises by assuming the time-dependence of the form $e^{i\omega t}$ in a transport equation. The exact solution to (3.21) is a right-traveling plane wave

$$\rho(x) = \rho_0 e^{-ikx}.$$

3.1. Purely spectral formulation. The spectral case is the easiest to describe because we can work with “non-broken” spaces and there is just one unknown flux. Set the test space $V = H^1(0, 1)$. The spectral variational formulation associated with (3.21) is

$$\begin{cases} \text{Find } (\rho, \hat{\rho}) \in U := L^2(0, 1) \times \mathbb{C}, \text{ such that :} \\ \underbrace{\int_0^1 -\rho(\overline{ikq + q'}) + \hat{\rho}\overline{q(1)}}_{b((\rho, \hat{\rho}), q)} = \rho_0 \overline{q_1(0)}, \quad \forall q \in V := H^1(0, 1). \end{cases} \quad (3.22)$$

Note the presence of the flux unknown $\hat{\rho}$.

As we saw in section 2.2, the choice of the norm in the trial space U determines the optimal norm and inner product on the test space V . We choose

$$\|(\rho, \hat{\rho})\|_U^2 := \|\rho\|_{L^2(0, 1)}^2 + |\hat{\rho}|^2,$$

as we would like the discrete solution to converge in L^2 . The optimal test norm defined by (2.4) is then

$$\|q\|_V = \sup_{(\rho, \hat{\rho}) \in U} \frac{|b((\rho, \hat{\rho}), q)|}{\|(\rho, \hat{\rho})\|_U}.$$

This supremum is immediately verified to be

$$\|q\|_V^2 = \|ikq + q'\|_{L^2(0, 1)}^2 + |q(1)|^2. \quad (3.23)$$

The inner product which generates this norm is also obvious:

$$(q, \delta q)_V = (ikq + q', ik\delta q + \delta q')_{L^2(0, 1)} + q(1)\overline{\delta q(1)}. \quad (3.24)$$

Next, we pick a trial space discretization. To obtain a spectral method, we can simply set

$$U_N \equiv U_p := P_p(0, 1) \times \mathbb{C}$$

where $P_p(0, 1)$ denotes the space of (complex) polynomials of degree at most p on $(0, 1)$. Then $V_N \equiv V_p$ is obtained as in (2.6) once we specify what T is for this example. For each e in U_N , the function $q = Te$ in V solves:

$$\begin{cases} \text{Find } q \equiv Te \in V \text{ such that:} \\ (ikq + q', ik\delta q + \delta q')_{L^2(0,1)} + q(1)\overline{\delta q(1)} = b(e, \delta q) \quad \forall \delta q \in V. \end{cases} \quad (3.25)$$

With U_p and V_p thus defined, our spectral DPG approximation of 3.21, namely $(\rho_p, \hat{\rho}_p) \in U_p$, is obtained by solving (2.7). By Proposition 2.1,

$$\begin{aligned} \|\rho - \rho_p\|_{L^2(0,1)}^2 + |\hat{\rho} - \hat{\rho}_p|^2 &= \inf_{(w_p, \hat{w}_p) \in U_p} \|\rho - w_p\|_{L^2(0,1)}^2 + |\hat{\rho} - \hat{w}_p|^2 \\ &= \inf_{w_p \in U_p} \|\rho - w_p\|_{L^2(0,1)}^2, \end{aligned} \quad (3.26)$$

i.e., the discrete solution ρ_p coincides with the $L^2(0, 1)$ -orthogonal projection of the exact solution ρ into the polynomial space. Moreover, $\hat{\rho} = \hat{\rho}_p$.

3.2. An intermediate method. We now modify the above spectral method in two steps: First, we set U_N to a discrete space of discontinuous functions based on a mesh (since the trial space of the formulation (3.22) is based in L^2 , this results in minimal modifications.) Partition $(0, 1)$ into n elements using

$$0 = x_0 < x_1 < \dots < x_{j-1} < x_j < \dots < x_n = 1. \quad (3.27)$$

Setting polynomial degrees p_j on each element $K_j = (x_{j-1}, x_j)$, define

$$\begin{aligned} L_{hp}^2 &:= \{w : w|_{K_j} \in P_{p_j}(K_j)\}, \\ U_N \equiv \check{U}_{hp} &:= L_{hp}^2 \times \mathbb{C}. \end{aligned} \quad (3.28)$$

The second modification is to change the inner product on V from (3.24) to

$$(q, \delta q)_{\tilde{V}} = (ikq + q', ik\delta q + \delta q')_{L^2(0,1)} + \frac{1}{2}(q, \delta q)_{L^2(0,1)}. \quad (3.29)$$

Lemma 3.1. *The norm $\|q\|_{\tilde{V}}$ generated by the above inner product is equivalent to the optimal V -norm in (3.23), i.e., (2.14) holds for all v in $H^1(0, 1)$ with*

$$C_1 = (2 - \sqrt{2})^{\frac{1}{2}}, \quad C_2 = (2 + \sqrt{2})^{\frac{1}{2}}.$$

The proofs of all lemmas, including this, can be found in the appendices. The reason for considering the modified \tilde{V} -inner product will be clear in § 3.3. We say that q is a *global optimal test function* for problem (3.21) if it is the optimal test function corresponding to some $(\rho, \hat{\rho}) \in \check{U}_{hp}$ in this setting, i.e.,

$$q \in H^1(0, 1) : \quad (q, \delta q)_{\tilde{V}} = \int_0^1 -\rho(\overline{ik\delta q + \delta q'}) + \hat{\rho}\overline{\delta q(1)}, \quad \forall \delta q \in H^1(0, 1). \quad (3.30)$$

We set V_N to \check{V}_{hp} , the span of all such global optimal test functions corresponding to all $(\rho, \hat{\rho}) \in \check{U}_{hp}$. We define an “intermediate method” for theoretical purposes, as follows:

$$\begin{cases} \text{Find } (\check{\rho}_{hp}, \hat{\rho}_{hp}) \in \check{U}_{hp} \text{ such that :} \\ \int_0^1 -\check{\rho}_{hp}(\overline{ikq + q'}) + \hat{\rho}\overline{q(1)} = \rho_0\overline{q_1(0)}, \quad \forall q \in \check{V}_{hp}. \end{cases} \quad (3.31)$$

Theorem 3.1. *We have the error estimate (with wave number independent constant)*

$$\|\rho - \check{\rho}_{hp}\|_{L^2(0,1)} \leq \left(\frac{2 + \sqrt{2}}{2 - \sqrt{2}} \right)^{\frac{1}{2}} \inf_{w_{hp} \in L^2_{hp}} \|\rho - w_{hp}\|_{L^2(0,1)}.$$

Proof. Apply Theorem 2.1 (its assumption is verified by Lemma 3.1). \square

3.3. The DPG method. The difficulty with the above defined intermediate method is that the computation of the optimal test space by (3.30) is a global problem, due to the global H^1 -conformity of the test space. To move to a more practical method, we now “break” the test space using the mesh (3.27), namely set

$$V = V_{\text{DPG}} = \prod_{j=1}^n V(K_j), \quad V(K_j) := H^1(x_{j-1}, x_j),$$

i.e., the test functions now have the form $q = (q_1, \dots, q_n) \in V_{\text{DPG}}$, where $q_j \in H^1(x_{j-1}, x_j)$. With this we can now state the DPG variational formulation of (3.21):

$$\begin{cases} \text{Find } (\rho, \hat{\rho}) \in U := L^2(0,1) \times \mathbb{C}^n \text{ such that :} \\ \sum_{j=1}^n \underbrace{\int_{x_{j-1}}^{x_j} -\rho(\overline{ikq_j + q'_j}) + \hat{\rho}_j \overline{[q]}_j = \rho_0 \overline{q_1(0)}}_{b((\rho, \hat{\rho}), q)}, \quad \forall q \in V_{\text{DPG}}, \end{cases} \quad (3.32)$$

where we have introduced the jumps defined by

$$[q]_j = \begin{cases} q_j(x_j) - q_{j+1}(x_j) & \text{if } j = 1, \dots, n-1, \\ q_n(1) & \text{if } j = n, \end{cases}$$

and the vector $\hat{\rho} = (\hat{\rho}_1, \dots, \hat{\rho}_n)$ of fluxes at element interfaces.

We choose the following norm on U :

$$\|(\rho, \hat{\rho})\|_U^2 = \|\rho\|_{L^2(0,1)}^2 + \sum_{j=1}^n |\hat{\rho}_j|^2.$$

Then, similar to the spectral case, an explicit expression of the optimal test norm is easily found:

$$\|q\|_{V_{\text{DPG}}}^2 = \sum_{j=1}^n \|ikq_j + q'_j\|_{L^2(x_{j-1}, x_j)}^2 + |[q]_j|^2. \quad (3.33)$$

The above norm is induced by the inner product

$$(q, \delta q)_{V_{\text{DPG}}} = \sum_{j=1}^n (ikq_j + q'_j, ik\delta q_j + \delta q'_j)_{L^2(x_{j-1}, x_j)} + [q]_j \overline{[\delta q]_j}.$$

Obviously, the norm above does not satisfy the localization property (2.19). We wish to replace it with a norm that does, in order to locally compute optimal test functions and obtain local error indicators. We use the norm (and associated inner product) given by:

$$\begin{aligned} \|q\|_{\tilde{V}}^2 &= \sum_{j=1}^n \|ikq_j + q'_j\|_{L^2(K_j)}^2 + \frac{1}{2} \|q_j\|_{L^2(K_j)}^2 \\ (q, \delta q)_{\tilde{V}} &= \sum_{j=1}^n (ikq_j + q'_j, ik\delta q_j + \delta q'_j)_{L^2(K_j)} + \frac{1}{2} (q_j, \delta q_j)_{L^2(K_j)}. \end{aligned} \quad (3.34)$$

Note that this is the same norm as in (3.29), when applied to q in $H^1(0,1)$.

The optimal test space is computed with the above \tilde{V} -inner product and the following discrete trial space

$$U_{hp} = L^2_{hp} \times \mathbb{C}^n \subset U$$

where L^2_{hp} is as defined in (3.28). Let $\{\rho_\ell\}$ denote the basis for L^2_{hp} consisting of functions each of which are supported only one element. Then a basis for U_{hp} takes the form (ρ_ℓ, \hat{e}_m) where $\{\hat{e}_1, \dots, \hat{e}_n\}$ denote the standard unit basis for \mathbb{C}^n . The corresponding optimal test functions can now be computed locally (unlike (3.30)), so we call them the *local optimal test functions*. If ρ_ℓ is supported on K_j , then the local optimal test function q for the trial basis $(\rho_\ell, 0)$ is supported solely on K_j and is computed by solving

$$(ikq + q', ik\delta q + \delta q')_{L^2(K_j)} + \frac{1}{2}(q, \delta q)_{L^2(K_j)} = \int_{x_{j-1}}^{x_j} -\rho_\ell(ik\delta q + \delta q'), \quad \forall \delta q \in V(K_j).$$

Similarly, the local optimal test function corresponding to the trial basis $(0, \hat{e}_j)$ is supported on $K_j \cup K_{j+1}$ and is obtained by solving

$$\begin{aligned} (ikq_j + q'_j, ik\delta q_j + \delta q'_j)_{L^2(K_j)} + \frac{1}{2}(q_j, \delta q_j)_{L^2(K_j)} &= \delta q_j(x_j), \\ (ikq_{j+1} + q'_{j+1}, ik\delta q_{j+1} + \delta q'_{j+1})_{L^2(K_{j+1})} + \frac{1}{2}(q_{j+1}, \delta q_{j+1})_{L^2(K_{j+1})} &= -\delta q_{j+1}(x_j), \end{aligned}$$

for all δq in V_{DPG} . We set the test space V_N to V_{hp} , the span of these optimal test functions. Clearly $V_{hp} \subseteq V_{DPG}$. The DPG method is then given as follows.

$$\left\{ \begin{array}{l} \text{Find } (\rho_{hp}, \hat{\rho}^{hp}) \in U_{hp} \text{ such that :} \\ \sum_{j=1}^n \int_{x_{j-1}}^{x_j} -\rho_{hp}(ikq_j + q'_j) + \hat{\rho}_j^{hp}\overline{[q]}_j = \rho_0 \overline{q_1(0)}, \quad \forall q \in V_{hp}. \end{array} \right. \quad (3.35)$$

We analyze this method using the following lemma, proved in Appendix A.

Lemma 3.2. *The global optimal test functions in \check{V}_{hp} are contained in V_{hp} . Consequently the solutions $\check{\rho}_{hp}$ of (3.31) and ρ_{hp} of (3.35) coincide:*

$$\check{\rho}_{hp} = \rho_{hp}.$$

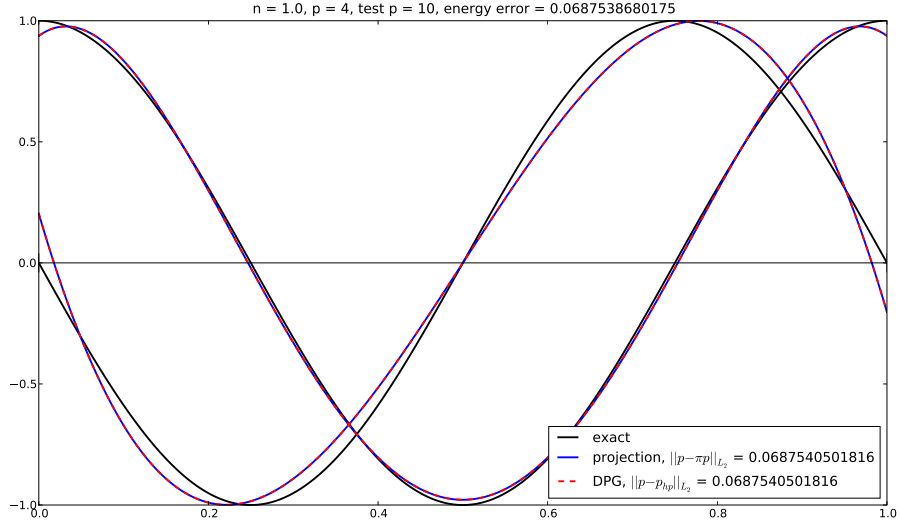
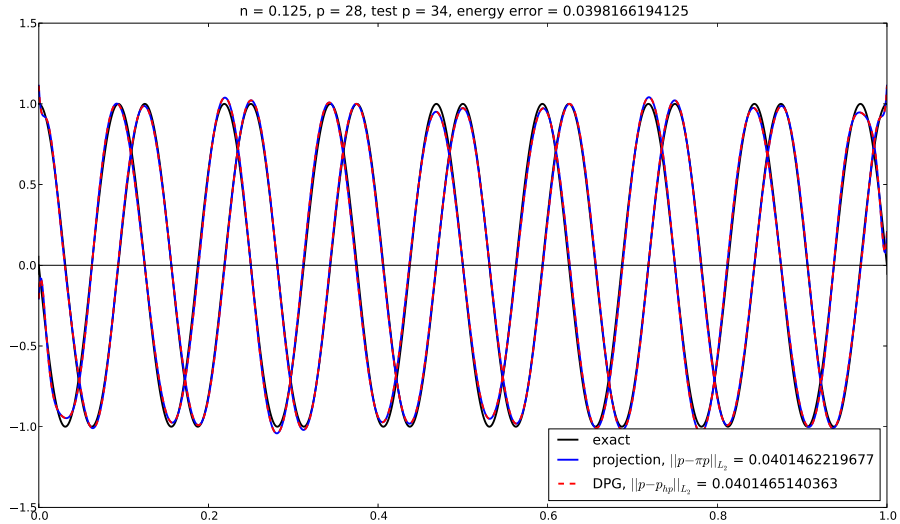
Theorem 3.2. *An error estimate holds with a constant independent of wave number:*

$$\|\rho - \rho_{hp}\|_{L^2(0,1)} \leq \left(\frac{2 + \sqrt{2}}{2 - \sqrt{2}} \right)^{\frac{1}{2}} \inf_{w_{hp} \in L^2_{hp}} \|\rho - w_{hp}\|_{L^2(0,1)}. \quad (3.36)$$

Proof. By Lemma 3.2, $\rho_{hp} = \check{\rho}_{hp}$, so (3.36) follows immediately from Theorem 3.1. \square

3.4. Numerical results. As noted in Section 2.5, we rely on higher order approximation in order to approximate the optimal test functions spanning the discrete test space V_{hp} . More precisely, corresponding to our trial space U_{hp} , we form an enriched test space $V_{hp}^+ \subset V$ from which we approximate the optimal test functions. Given an element K on the interval (x_{j-1}, x_j) in our mesh of polynomial order p , its discrete enriched local test space $V_{hp}^+(K) \subset H^1(x_{j-1}, x_j)$ is formed by the span of polynomials of order $p + \Delta p$, for $\Delta p \geq 1$. The local test space $V_{hp}(K) \subset V(K)$ is determined by solving the discrete local problems

$$\left\{ \begin{array}{l} \text{Find } q_{hp} \in V_{hp}^+(K) \text{ such that:} \\ (q_{hp}, \delta q)_V = b_K(e, \delta q) \quad \forall \delta q \in V_{hp}^+(K) \end{array} \right.$$

(a) One wavelength, $p = 4$ (b) Eight wavelengths, $p = 28$ Figure 1: Results for spectral method on one element; $\Delta p = 6$

for each trial basis function $e \in U_{hp}$ supported in element K . Here $b_K(\cdot, \cdot)$ denotes the localized sesquilinear form, defined for $q \in V(K_j)$ by

$$b_K((p, \hat{\rho}), q) := \begin{cases} \int_K -p(\overline{ikq + q'}) + \hat{\rho}_j q(x_j) - \hat{\rho}_{j-1} q(x_{j-1}) & j > 1, \\ \int_K -p(\overline{ikq + q'}) + \hat{\rho}_j q(x_j) & j = 1. \end{cases} \quad (3.37)$$

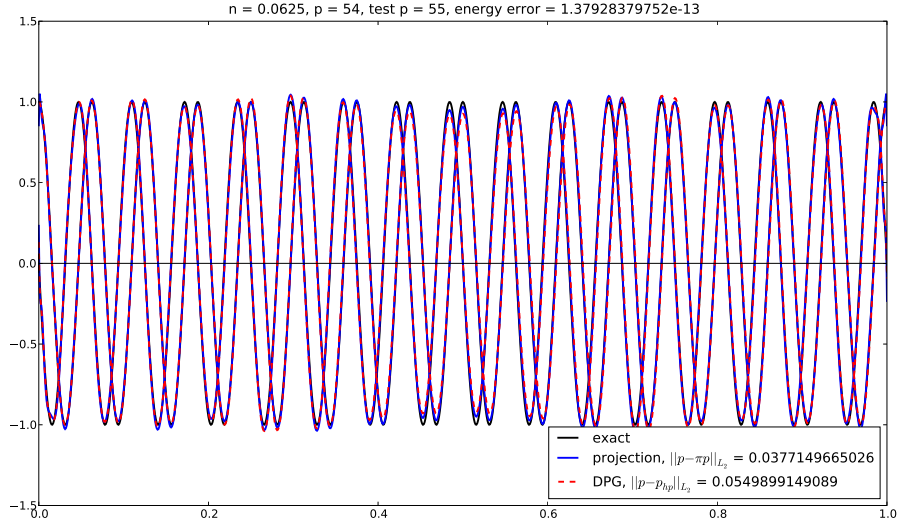


Figure 2: Degraded performance with insufficiently enriched test space: $\Delta p = 1$

In all of the following examples, we take $p_0 = 1$ in (3.21). We begin with the one element case, where there is no distinction between the spectral and DPG methods. Given an element of order p , the order $p + \Delta p$ of the enriched discrete test space V_{hp}^+ is taken using $\Delta p = 6$. As the results (Figures 1a-1b) demonstrate, this is sufficient to realize practically perfect L_2 stability for the considered wavenumbers; the L_2 projected and DPG solutions are visually indistinguishable, and the L_2 error of the DPG solution is within 10^{-6} percent of the projection.

Lowering the enrichment Δp of the enriched test space results in a gradual degradation in performance until the dimensions of the trial and enriched space are equal (Fig. 2.) The optimal test functions exhibit oscillations of the problem wavelength k , so it is to be expected that without sufficient order $p + \Delta p$ of the enriched test space, we are unable to approximate them well enough to obtain the desired stability.

For the DPG setting, we employ the localizable inner product (3.34). Re-examining the spectral case with the modified inner product indicates that we retain excellent stability (Fig. 3). Figures 4a-4b show results obtained with four linear elements per wavelength, for one and 16 wavelengths over the length of the domain, respectively. We observe very good L_2 stability, regardless of wavenumber, as illustrated in Fig. 5.

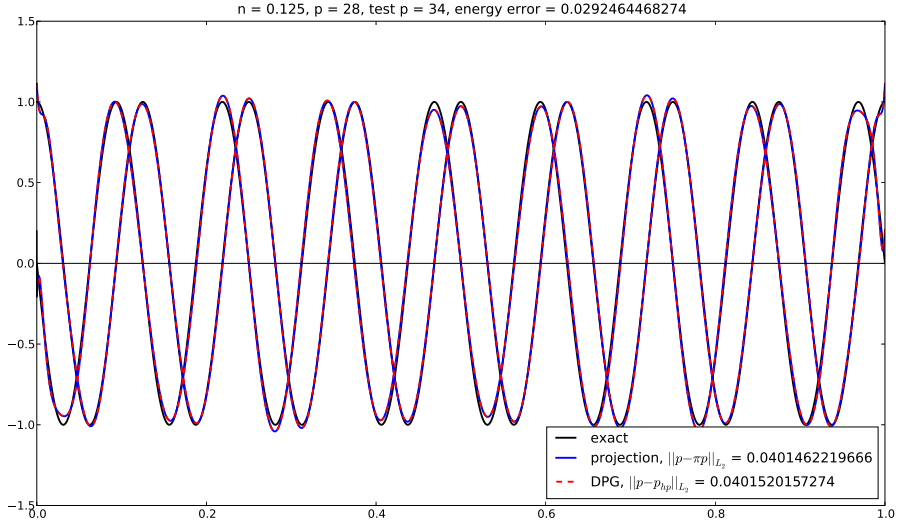


Figure 3: Eight wavelengths, $p = 28$, localizable inner product

4. THE HELMHOLTZ MODEL PROBLEM

In this section, we study the coupled Helmholtz problem in 1D, represented in terms of *pressure* p and *velocity* u , coupled in a system of first-order differential equations. Again, we demonstrate that with a proper choice of the norm for the test functions, the stability properties turn out to be *wavenumber-independent*. We start by analyzing the spectral problem and we prove robustness of the method in this simple setting. Then we introduce the DPG formulation that delivers the same FE solution as the spectral one, when using the same trial FE basis. Hence, the robustness result will apply to the DPG solution as well.

4.1. The variational equations. We consider the Helmholtz equation written as a system of two first order equations. The new unknowns have physical meaning, e.g., in the theory of acoustical disturbances [7]. Given an inflow data $u_0 \in \mathbb{C}$, the speed of sound c , and the density of the fluid ρ , we consider the boundary value problem

$$\begin{cases} ik \frac{p}{c\rho} + u' = 0 & \text{in } \Omega = (0, 1), \\ ik c\rho u + p' = 0 & \text{in } \Omega = (0, 1), \\ u(0) = u_0 & \text{and} \\ p(1) = Zu(1), & \end{cases} \quad (4.38)$$

where Z is an impedance parameter relating p and u at the right side boundary. The choice $Z = c\rho$ leads to the exact right-traveling wave solution

$$u(x) = u_0 e^{-ikx}, \quad p(x) = c\rho u(x).$$

For the sake of simplicity, we will just consider the values $Z = c\rho = 1$.

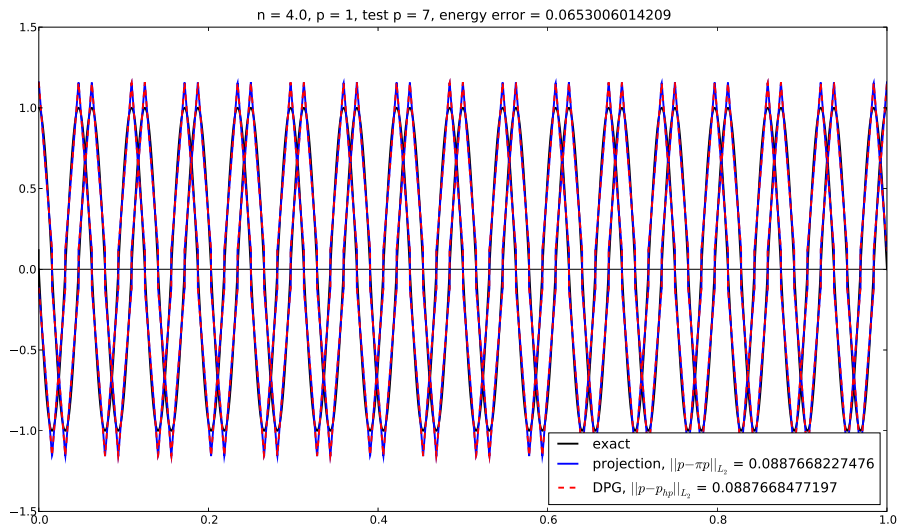
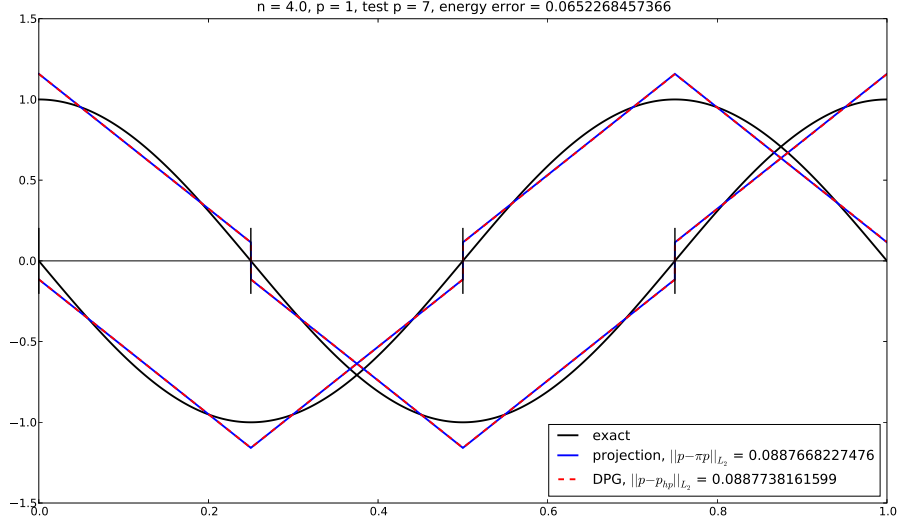


Figure 4: Localizable inner product; four linear elements per wavelength

In the context of an *unbroken* test space, the natural variational formulation associated with (3.21) is

$$\left\{ \begin{array}{l} \text{Find } (p, u, \hat{p}_0, \hat{u}_1) \in U := [L^2(\Omega)]^2 \times \mathbb{C}^2, \text{ such that :} \\ ik \int_{\Omega} p \bar{q} - \int_{\Omega} u \bar{q}' + \hat{u}_1 \bar{q}(1) = u_0 \bar{q}(0), \\ ik \int_{\Omega} u \bar{v} - \int_{\Omega} p \bar{v}' + \hat{u}_1 \bar{v}(1) - \hat{p}_0 \bar{v}(0) = 0, \quad \forall (q, v) \in V := [H^1(\Omega)]^2. \end{array} \right. \quad (4.39)$$

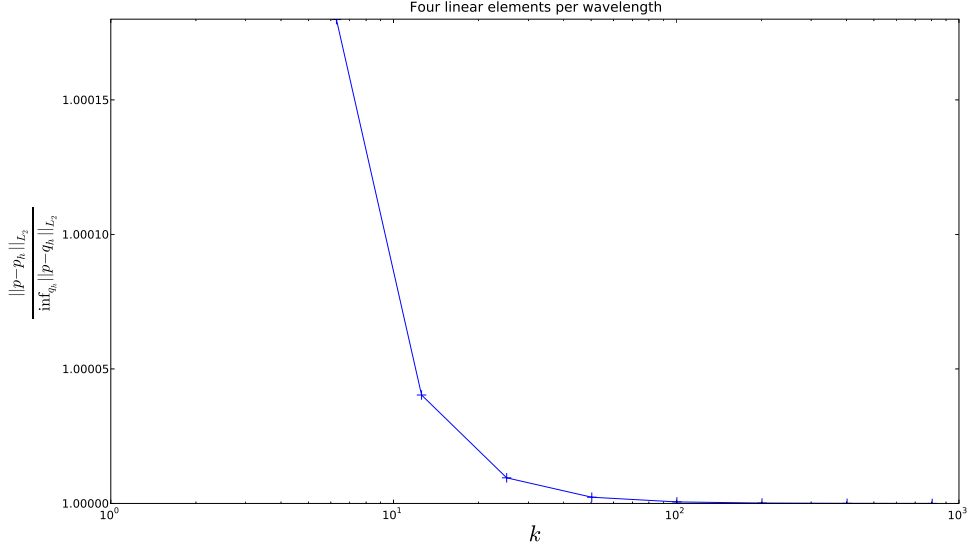


Figure 5: Adhering to a fixed number of elements per wavelength is sufficient to control stability under the localizable norm.

As in § 3.1, this will immediately lead to a spectral method, once we select the trial space norm in which we would like convergence, i.e.,

$$\|p, u, \hat{p}_0, \hat{u}_1\|_U^2 := \|p\|_{L^2}^2 + \|u\|_{L^2}^2 + |\hat{p}_0|^2 + |\hat{u}_1|^2.$$

Then, the sesquilinear form on the left side of (4.39) yields the following *optimal inner product and norm* on V :

$$\begin{aligned} ((q, v), (\delta q, \delta v))_V &= (ikq + v', ik\delta q + \delta v')_{L^2} + (ikv + q', ik\delta v + \delta q')_{L^2} \\ &\quad + (q(1) + v(1))(\bar{\delta q}(1) + \bar{\delta v}(1)) + v(0)\bar{\delta v}(0) \end{aligned} \tag{4.40}$$

$$\|q, v\|_V^2 = \|ikq + v'\|_{L^2}^2 + \|ikv + q'\|_{L^2}^2 + |q(1) + v(1)|^2 + |v(0)|^2.$$

Inspired by what we have observed in the previous section, we replace (4.40) with the following localizable norm (and associated inner product):

$$\begin{aligned} \|q, v\|_{\tilde{V}}^2 &= \|ikq + v'\|_{L^2}^2 + \|ikv + q'\|_{L^2}^2 + \frac{1}{\alpha} \|v + q\|_{L^2}^2 + \frac{1}{\alpha} \|v \cos(kx) + iq \sin(kx)\|_{L^2}^2 \\ ((q, v), (\delta q, \delta v))_{\tilde{V}} &= (ikv + q', ik\delta v + \delta q')_{L^2} + (ikq + v', ik\delta q + \delta v')_{L^2} + \frac{1}{\alpha} (v + q, \delta v + \delta q)_{L^2} \\ &\quad + \frac{1}{\alpha} (v \cos(kx) + iq \sin(kx), \delta v \cos(kx) + i\delta q \sin(kx))_{L^2}, \end{aligned} \tag{4.41}$$

where $\alpha = \frac{5+\sqrt{5}}{2}$. Then we have the norm equivalence result (2.14), as stated in the next lemma. Its proof is in Appendix A.

Lemma 4.1. *For all (q, v) in V ,*

$$C_1 \|(q, v)\|_{\tilde{V}}^2 \leq \|(q, v)\|_V^2 \leq C_2 \|(q, v)\|_{\tilde{V}}^2,$$

with constants $C_1 = \frac{5+\sqrt{5}}{2} - (5+2\sqrt{5})^{\frac{1}{2}}$ and $C_2 = \frac{5+\sqrt{5}}{2} + (5+2\sqrt{5})^{\frac{1}{2}}$.

The next step is to consider an “intermediate method” as in § 3.2. Again let (3.27) define the mesh of $(0, 1)$. The trial space in this case is $\check{U}_{hp} = [L^2_{hp}(\Omega)]^2 \times \mathbb{C}^2$. Let $\{(p_l, u_l, \hat{p}_l, \hat{u}_l)\}_{l=1,\dots,N} \subset [L^2(\Omega)]^2 \times \mathbb{C}^2$ be a finite trial basis such that each p_l and u_l are in L^2_{hp} and are supported on a single element. With these as the trial functions and (4.41) as the inner product, we find the corresponding optimal test functions. These are the *global optimal test functions* for this case and we denote their span by \check{V}_{hp} . Let $\check{\mathcal{U}}_{hp} = (p_{hp}, u_{hp}, \hat{p}_{hp}, \hat{u}_{hp})$ be the discrete solution from this method. Then we have the following robust error estimate for the intermediate problem.

Theorem 4.1. *Let $\check{\mathcal{U}} = (p, u, \hat{p}, \hat{u})$ be the exact solution of problem (4.39). Then*

$$\|\check{\mathcal{U}} - \check{\mathcal{U}}_{hp}\|_U \leq \left(\sqrt{\frac{5 + \sqrt{5}}{2}} + \sqrt{\frac{3 + \sqrt{5}}{2}} \right) \inf_{\mathcal{W}_{hp} \in \check{V}_{hp}} \|\check{\mathcal{U}} - \mathcal{W}_{hp}\|_U. \quad (4.42)$$

Proof. This follows from Theorem 2.1 and Lemma 4.1. \square

As before, the global optimal test functions are expensive to compute. Hence we formulate the DPG method with local optimal test functions next.

4.2. The DPG formulation. Using the same partition (3.27) of the interval $(0, 1)$, we formulate the DPG method as follows. The unknowns include field variables (p, u) and fluxes \hat{p}_{j-1}, \hat{u}_j , $j = 1, \dots, n$. Fluxes \hat{u}_0, \hat{p}_n were replaced by u_0 and \hat{u}_n respectively by using the boundary conditions. For each element (x_{j-1}, x_j) , we consider local test functions $(q_j, v_j) \in [H^1(x_{j-1}, x_j)]^2$. The DPG variational formulation is :

$$\begin{cases} \text{Find } (p, u, \hat{p}, \hat{u}) \in L^2(\Omega) \times L^2(\Omega) \times \mathbb{C}^n \times \mathbb{C}^n \text{ such that :} \\ \sum_{j=1}^n ik \int_{x_{j-1}}^{x_j} p \bar{q}_j - \int_{x_{j-1}}^{x_j} u \bar{q}'_j + (\hat{u} \bar{q}) \Big|_{x_{j-1}}^{x_j} = 0 \\ \sum_{j=1}^n ik \int_{x_{j-1}}^{x_j} u \bar{v}_j - \int_{x_{j-1}}^{x_j} p \bar{v}'_j + (\hat{p} \bar{v}) \Big|_{x_{j-1}}^{x_j} = 0, \quad \forall (q_j, v_j) \in [H^1(K_j)]^2. \end{cases} \quad (4.43)$$

Recall that $\hat{u}_0 = u_0$ is known and is moved to the right-hand side. Similarly, \hat{p}_n is replaced by \hat{u}_n in the last term of the sum. The *broken test space* in the variational formulation (4.43) is endowed with the norm and inner product induced by (4.41):

$$\begin{aligned} \|q, v\|_{\check{V}}^2 &= \sum_{j=1}^n \|ikq_j + v'_j\|_{L^2}^2 + \|ikv_j + q'_j\|_{L^2}^2 \\ &\quad + \frac{1}{\alpha} \sum_{j=1}^n \|v_j + q_j\|_{L^2}^2 + \|v_j \cos(kx) + iq_j \sin(kx)\|_{L^2}^2 \\ ((q, v), (\delta q, \delta v))_{\check{V}} &= \sum_{j=1}^n (ikv_j + q'_j, ik\delta v_j + \delta q'_j)_{L^2} + (ikq_j + v'_j, ik\delta q_j + \delta v'_j)_{L^2} \\ &\quad + \frac{1}{\alpha} \sum_{j=1}^n (v_j + q_j, \delta v_j + \delta q_j)_{L^2} \\ &\quad + \frac{1}{\alpha} \sum_{j=1}^n (v_j \cos(kx) + iq_j \sin(kx), \delta v_j \cos(kx) + i\delta q_j \sin(kx))_{L^2}. \end{aligned}$$

The discrete trial space is obtained by substituting L_{hp}^2 for $L^2(0, 1)$. The corresponding optimal test functions computed using the above \tilde{V} -inner product gives the *local optimal test functions*. Their span gives the test space V_{hp} which defines the full DPG method. Let $(p_{hp}, u_{hp}, \hat{p}_{hp}, \hat{u}_{hp})$ be the discrete solution.

Theorem 4.2. *The global optimal test functions are contained in the space of local optimal test functions. Consequently,*

$$\|u - u_{hp}\|_{L^2}^2 + \|p - p_{hp}\|_{L^2}^2 \leq \left(\sqrt{\frac{5 + \sqrt{5}}{2}} + \sqrt{\frac{3 + \sqrt{5}}{2}} \right)^2 \inf_{w_{hp}, s_{hp} \in L_{hp}^2} \|u - w_{hp}\|_{L^2}^2 + \|p - s_{hp}\|_{L^2}^2.$$

The proof of this theorem is similar to the proof of Theorem 3.2 (cf. proof of Lemma 3.2), so we omit it.

Based on the discussion made in Section 2.4, the robustness estimation (4.42) also applies for the FE solution of this formulation, under analog considerations of the discrete trial space, aside from the additional $2(n - 1)$ fluxes.

4.3. Numerical results. Figures 6a-6b depict results for the spectral method, taking $u_0 = 1$, $Z = 1$. Again we have taken $\Delta p = 6$ in constructing the enriched test space, which achieves nearly perfect L_2 stability. Only the pressures p are plotted; the error in the velocity u is practically identical.

The optimal test functions (q, v) in the spectral case may be expressed as the solutions of the problem:

$$\begin{cases} ikq + v' &= -p \quad \text{in } (0, 1), \\ ikv + q' &= -u \quad \text{in } (0, 1), \\ v(0) &= -\hat{p}_0, \\ q(1) + v(1) &= \hat{u}_1. \end{cases}$$

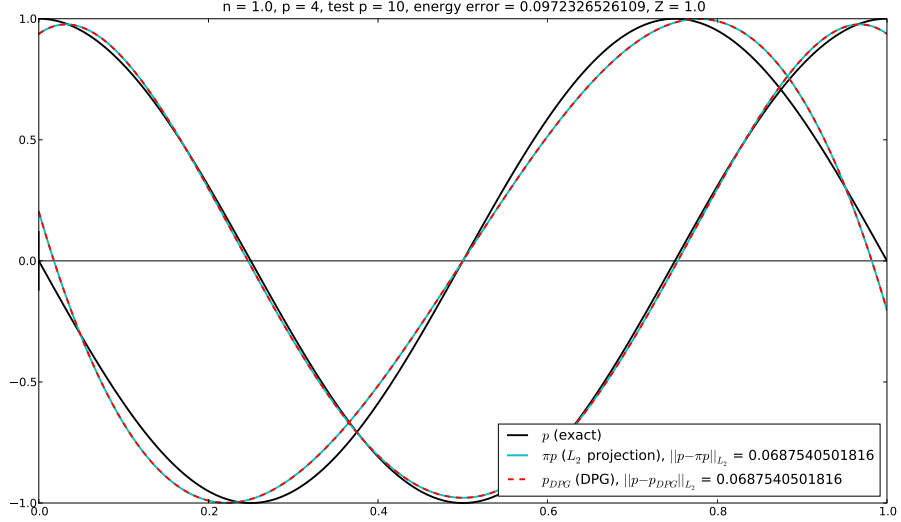
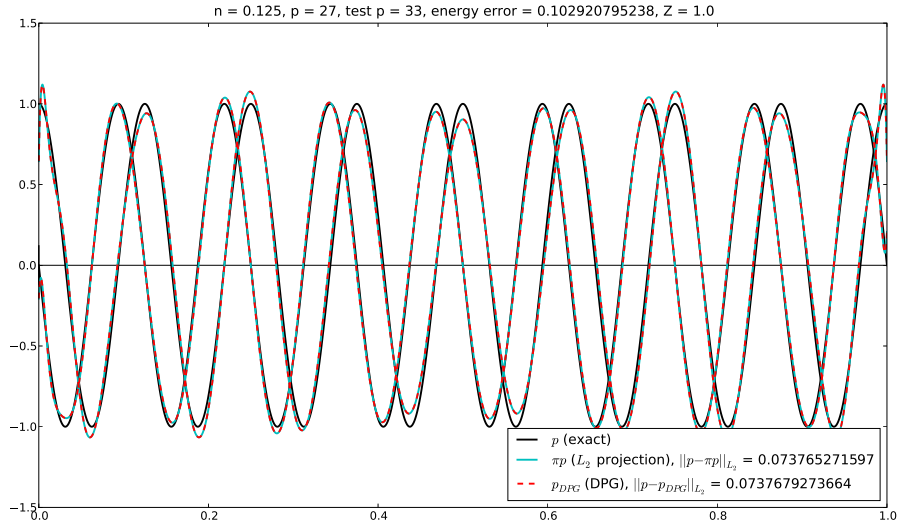
The optimal test functions for a number of basis functions are illustrated in Figures 7a-7d. Their oscillatory behavior corresponding to wavenumber k makes clear the necessity of using sufficient order $p + \Delta p$ within the enriched test space.

For the multi-element case, we employ the localizable norm (4.41). Corresponding optimal test functions are shown in Figures 8a-8d. Results obtained with the localizable norm are shown in Figures 9a-9b. Again, we observe excellent stability with the DPG method. In contrast to standard methods, there is no degradation in stability with increasing wavenumber; indeed, if we adhere to a “rule of thumb” of n elements per wavelength as we vary k , we observe that the stability constant converges to a k -independent value (Figures 10a-10b.) For comparison, we plot in Fig. 4.3 a standard H^1 -conforming, Bubnov-Galerkin approximation p_{hp} , as well as an H^1 -conforming approximation p_{blended} obtained using specialized quadrature rules which reduce the phase lag (see [1].) While they are obtained using the same discretization, i.e. order and number of elements, we must note that they only require solution of the pressure field p , while the DPG method requires the introduction of additional variables u , \hat{p} , and \hat{u} , requiring significantly more degrees of freedom.

Even at extremely poor discretization (e.g. 2 linear elements per wavelength), the method remains stable, delivering results very near the L_2 projection (Fig. 12).

Figures 13a-13b show results obtained with high-order elements ($p = 4$, $p = 8$).

4.4. Helmholtz with PML truncation. Finally, we consider the Helmholtz problem with PML truncation at the right end of the domain, admitting only outgoing and evanescent waves.

(a) One wavelength, $p = 4$ (b) 8 wavelengths, $p = 27$ Figure 6: Helmholtz spectral element; $\Delta p = 6$

We employ the PML stretching function

$$z(x) = \begin{cases} x & \text{in } (0, \ell) \\ x - i \frac{C}{k} \left(\frac{x-\ell}{1-\ell} \right)^4 + \frac{C}{k} \left(\frac{x-\ell}{1-\ell} \right)^4 & \text{in } (\ell, 1), \end{cases}$$

where ℓ is the position at which the PML begins, and C is a parameter controlling the strength of the PML (we take $C = 745$ to achieve decay to near machine epsilon (double precision) for a

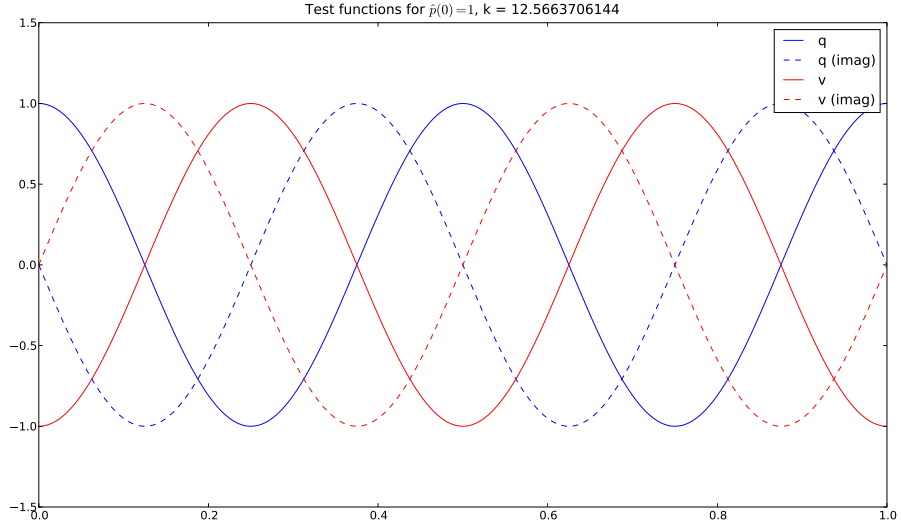
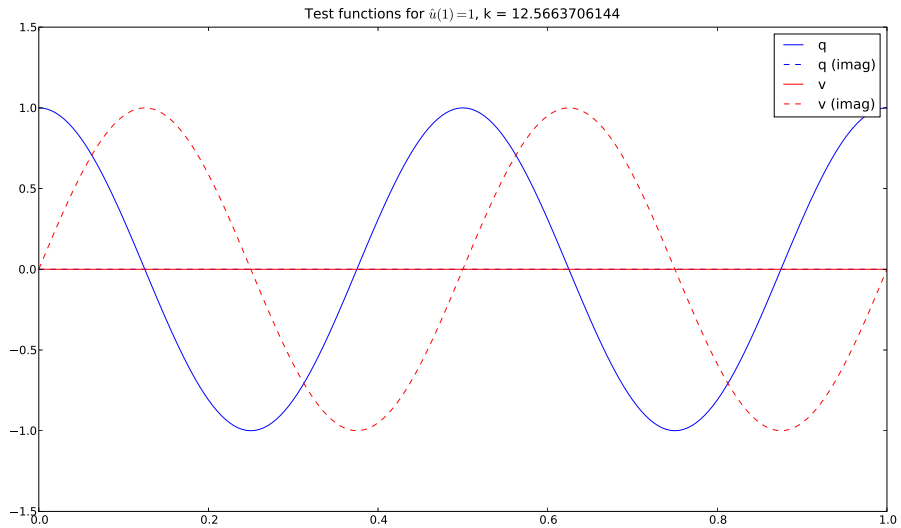
(a) Optimal test function for basis flux $\hat{p}_0 = 1$ (b) Optimal test function for basis flux $\hat{u}_1 = 1$

Figure 7: Optimal test functions for Helmholtz spectral element

plane wave of unit amplitude). The PML problem is then:

$$\begin{cases} ikz'p + u' = 0 & \text{in } \Omega = (0, 1), \\ ikz'u + p' = 0 & \text{in } \Omega = (0, 1), \\ u(0) = u_0, \\ p(1) = 0. \end{cases}$$

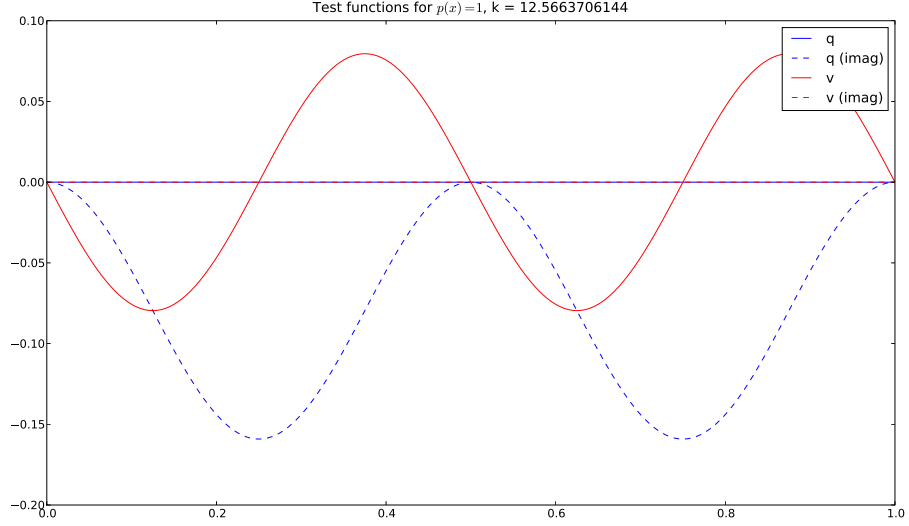
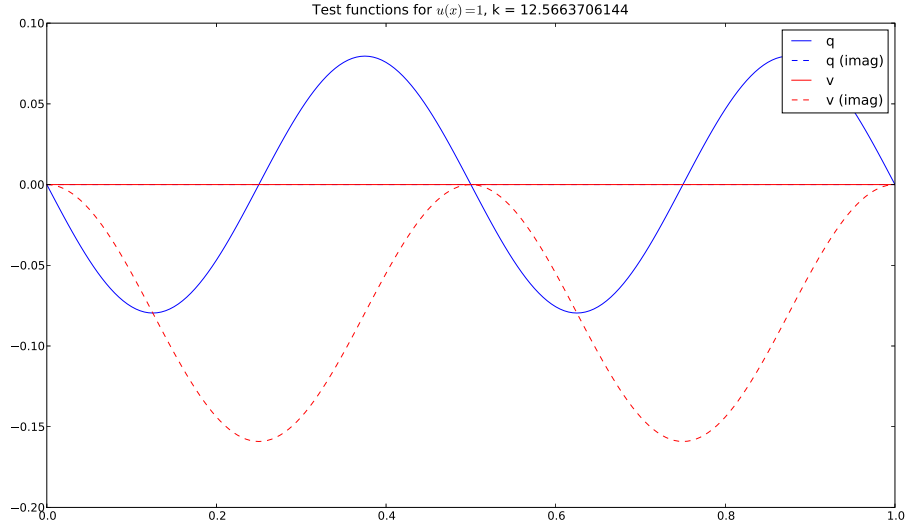
(c) Optimal test function for basis function $p(x) = 1$ (d) Optimal test function for basis function $u(x) = 1$

Figure 7: Optimal test functions for Helmholtz spectral element

The DPG variational formulation is:

Find $(p, u, \hat{\mathbf{p}}, \hat{\mathbf{u}}) \in L^2(0, 1) \times L^2(0, 1) \times \mathbb{C}^n \times \mathbb{C}^n$ such that:

$$\sum_{j=1}^n \int_{x_{j-1}}^{x_j} -p(\overline{ikz'q_j + v'_j}) - u(\overline{ikz'v_j + q'_j}) + \hat{u}_j \overline{[\mathbf{q}]_j} + \hat{p}_{j-1} \overline{[\mathbf{v}]_{j-1}} = u_0 q_1(0) \quad \forall (\mathbf{q}, \mathbf{v}) \in V_{\text{DPG}}.$$

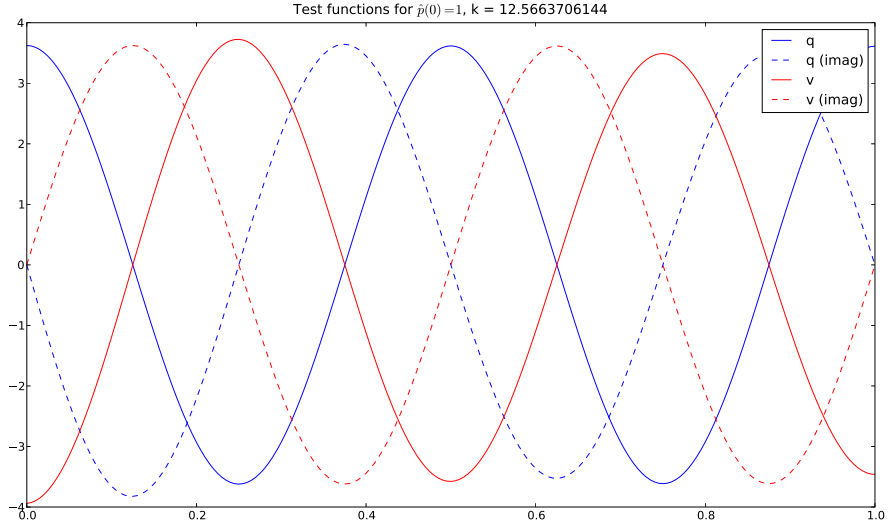
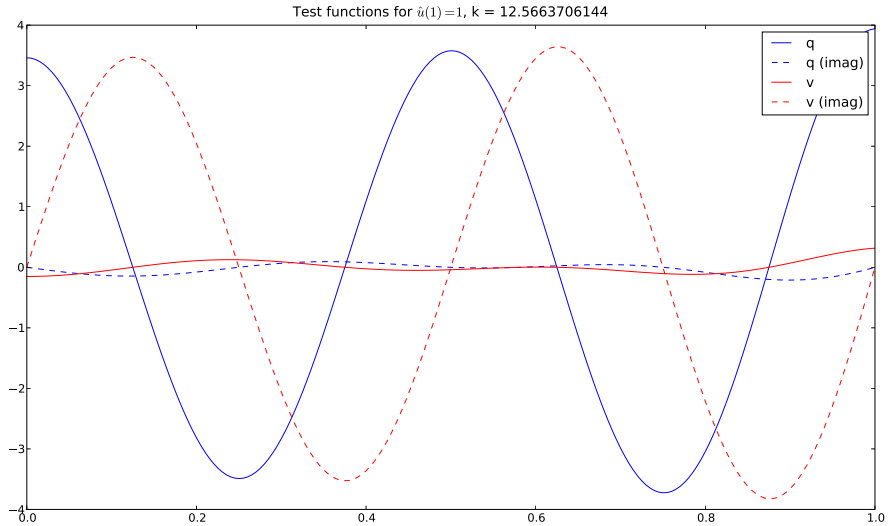
(a) Optimal test function for basis flux $\hat{p}_0 = 1$ (b) Optimal test function for basis flux $\hat{u}_1 = 1$

Figure 8: Optimal test functions for localizable norm

The optimal test norm is evidently:

$$\|\mathbf{q}, \mathbf{v}\|_{V_{\text{DPG}}} = \sum_{j=1}^n \|ikz' q_j + v'_j\|_{L^2(x_{j-1}, x_j)}^2 + \|ikz' v_j + q'_j\|_{L^2(x_{j-1}, x_j)}^2 + |[\mathbf{q}]_j|^2 + |[\mathbf{v}]_{j-1}|^2.$$

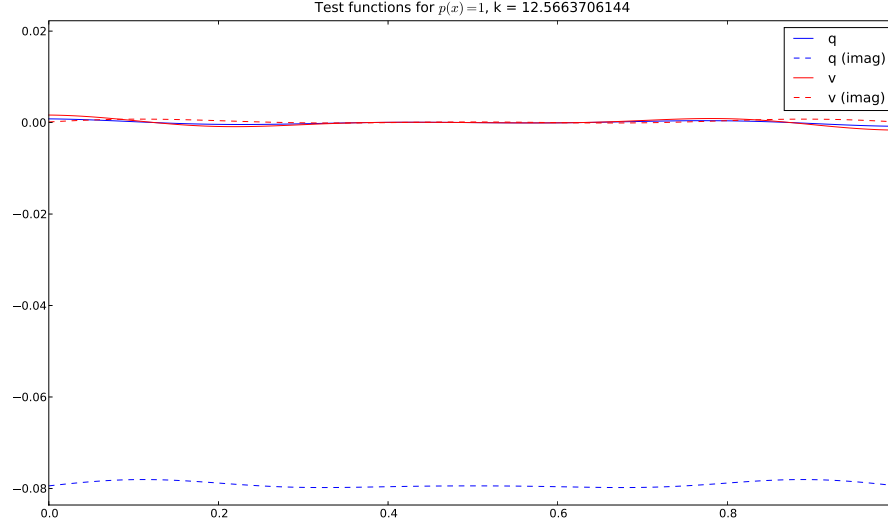
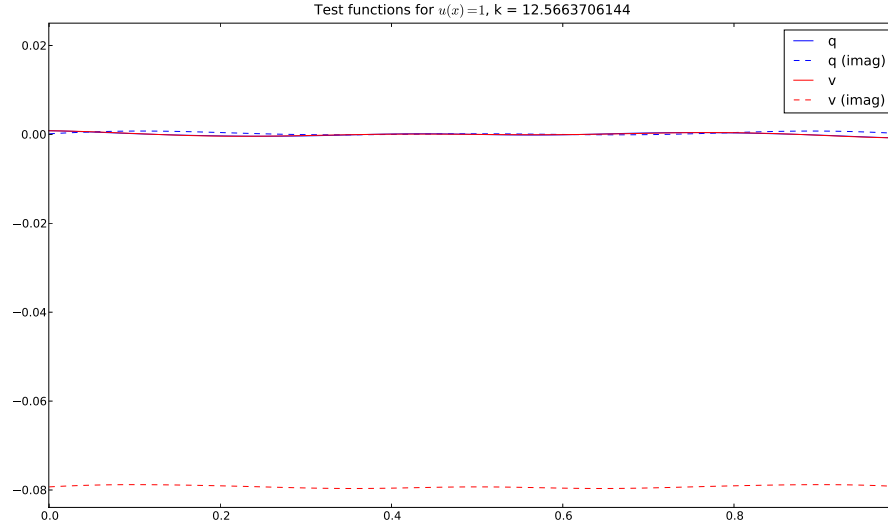
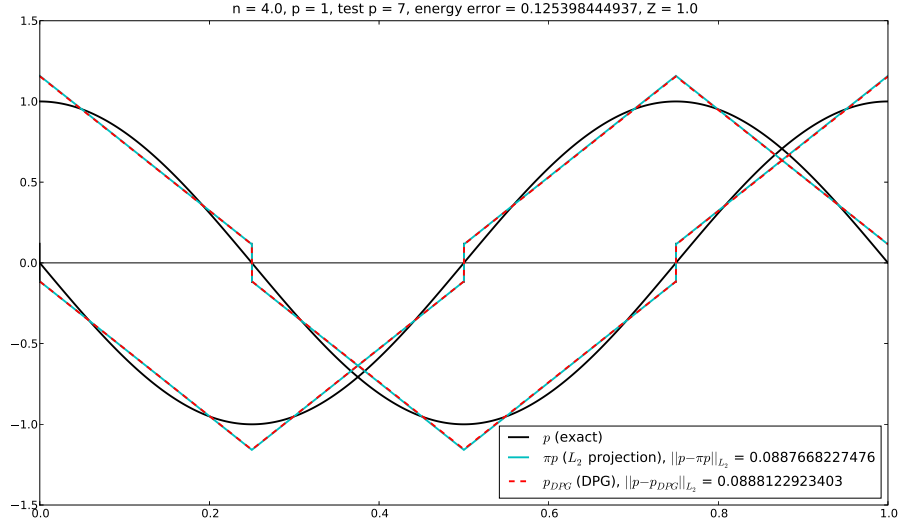
(c) Optimal test function for basis function $p(x) = 1$ (d) Optimal test function for basis function $u(x) = 1$

Figure 8: Optimal test functions for localizable norm

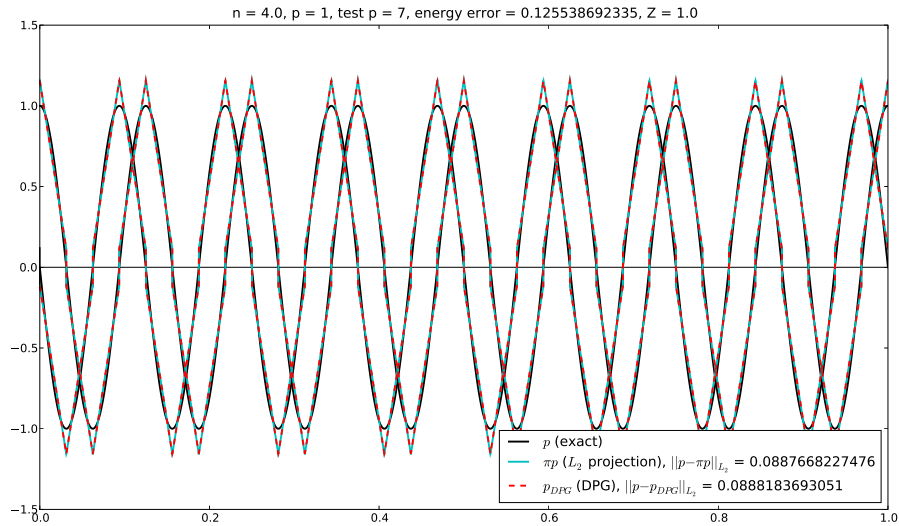
For multi-element computations, we employ an equivalent localizable norm:

$$\|\mathbf{q}, \mathbf{v}\|_{V_{\text{DPG}}} = \sum_{j=1}^n \|ikz'q_j + v'_j\|_{L^2(x_{j-1}, x_j)}^2 + \|ikz'v_j + q'_j\|_{L^2(x_{j-1}, x_j)}^2 + \|q_j\|_{L^2(x_{j-1}, x_j)}^2 + \|v_j\|_{L^2(x_{j-1}, x_j)}.$$

Evidently (Figures 14a-14b), we have to dramatically enrich our test space to realize in practice the optimal test functions delivering nearly perfect L_2 stability.



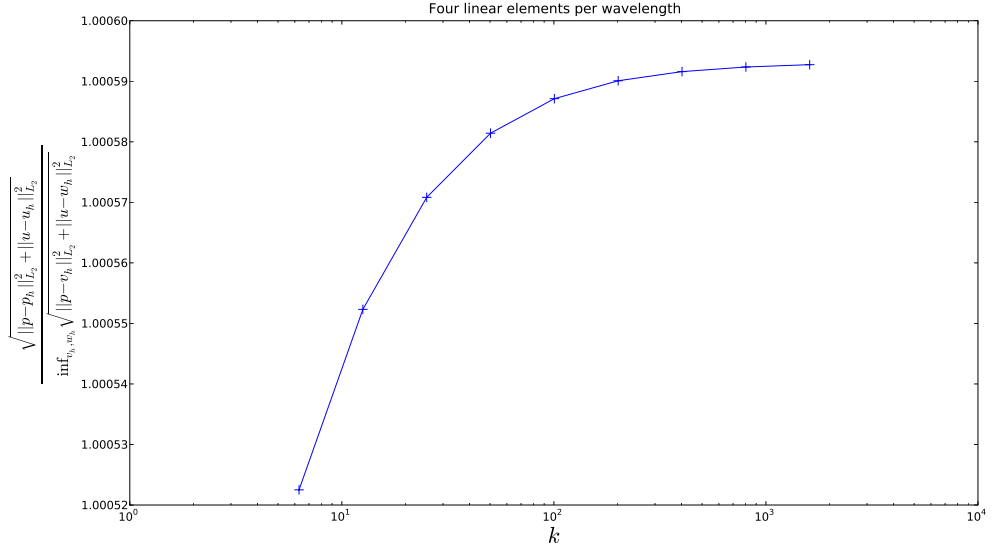
(a) One wavelength



(b) Eight wavelengths

Figure 9: Localizable inner product; four linear elements per wavelength

In Figures 15a-15b, the PML occupies only one linear element; in this extreme example, we must again take a very enriched test space to obtain test functions providing good stability. Figures 16a-17b demonstrate that less enrichment is necessary when better discretization is used within the PML.



(a) Four linear elements per wavelength

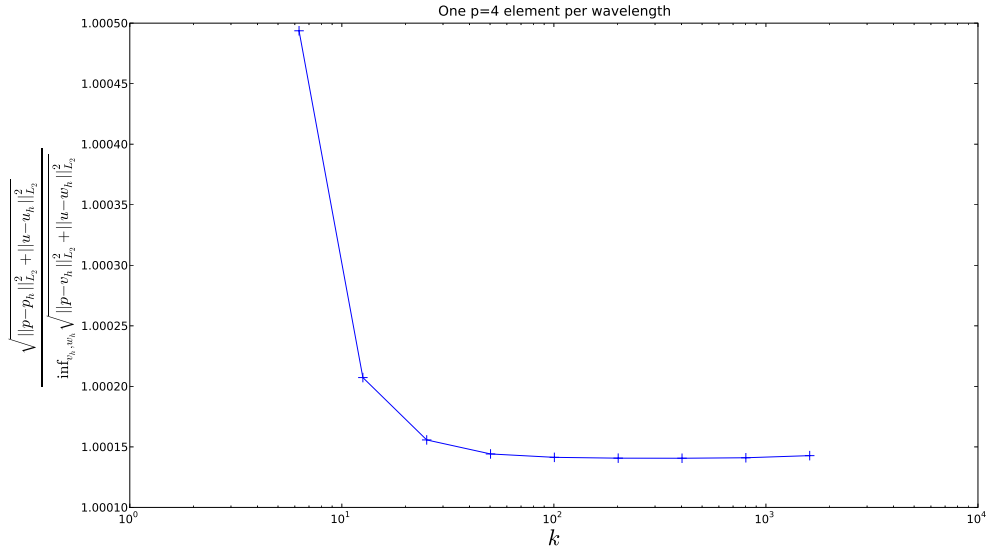
(b) One $p = 4$ element per wavelength

Figure 10: Adhering to a fixed number of elements per wavelength is sufficient to control stability under the localizable norm

5. CONCLUSIONS

A summary. With the introduction of the optimal test norm, an essential question of the whole framework of DPG with optimal test functions has been answered: given a norm on U in which we wish to minimize error, how does one design a norm on the test space V to induce the desired stability? The process includes a non-trivial “norm-localization” step, in which the optimal test

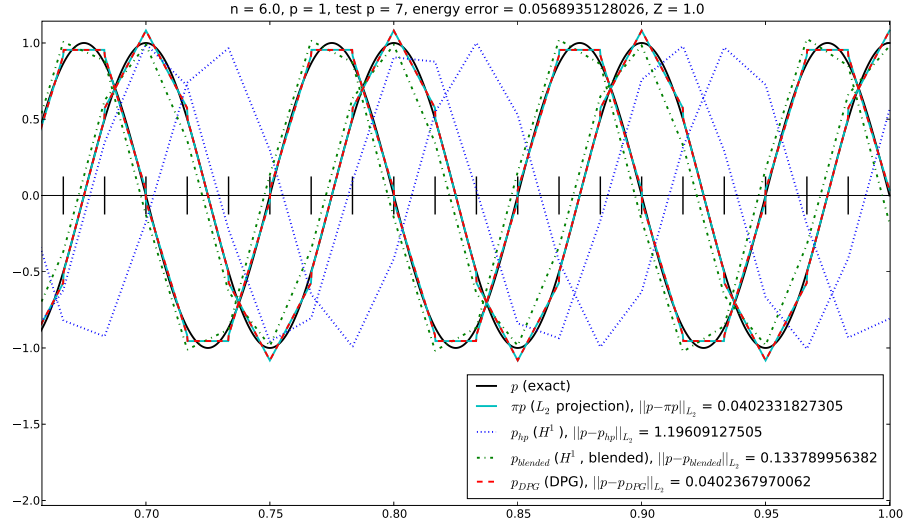


Figure 11: The standard H^1 conforming solution p_{hp} quickly exhibits excessive phase error; it is reduced but still present in $p_{blended}$

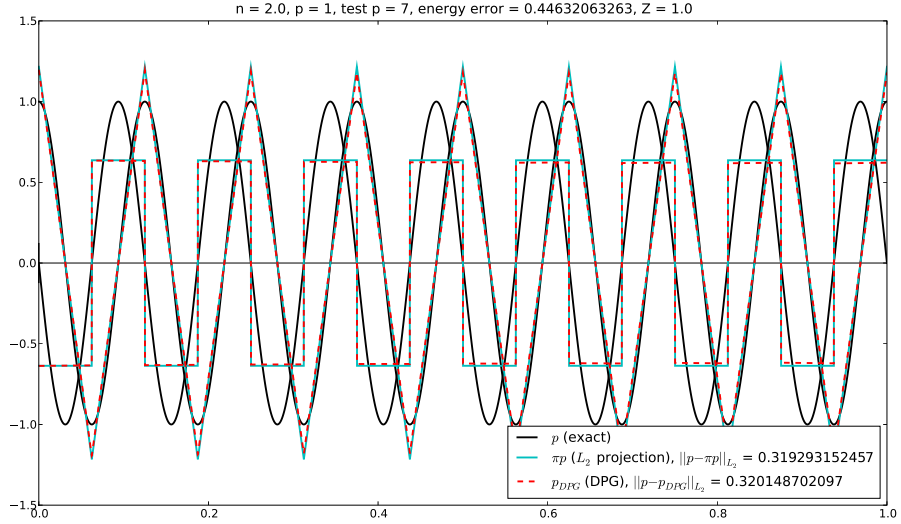


Figure 12: Two linear elements per wavelength

norm has to be replaced with a “localizable” norm, without losing uniform stability with respect to the wavenumber. The proposed methodology is very general, and applies to other singular perturbation problems. The leading term of the equations satisfied by the optimal test functions is the L^2 -adjoint of the original operator, resembling very much the old results of [22, 12, 18]. In context of singular perturbation problems, this means that the whole burden of dealing with

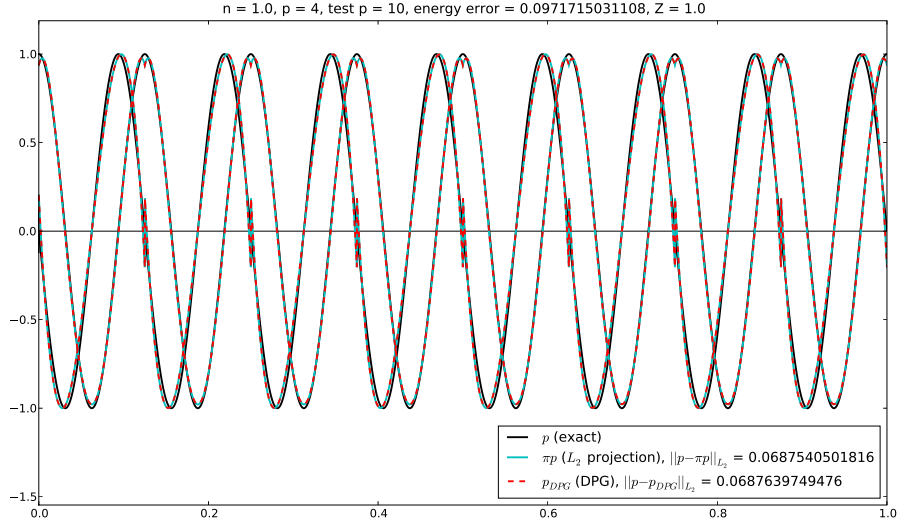
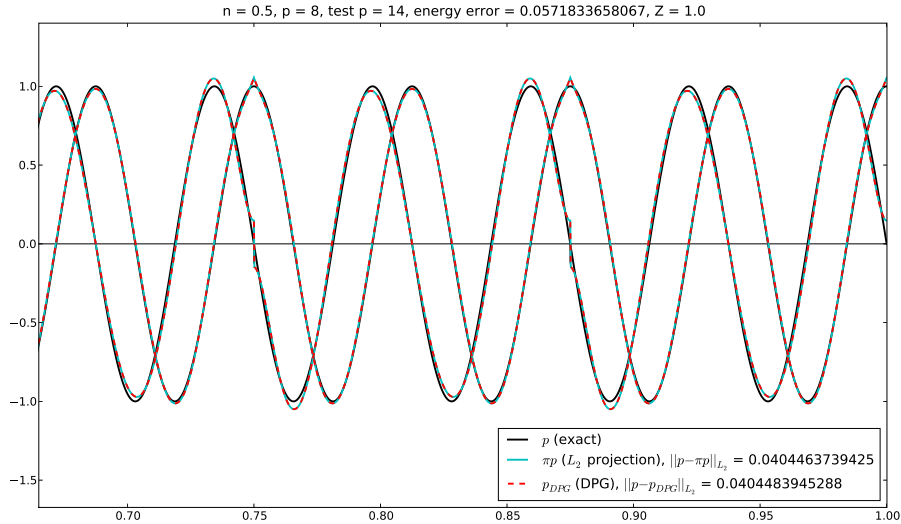
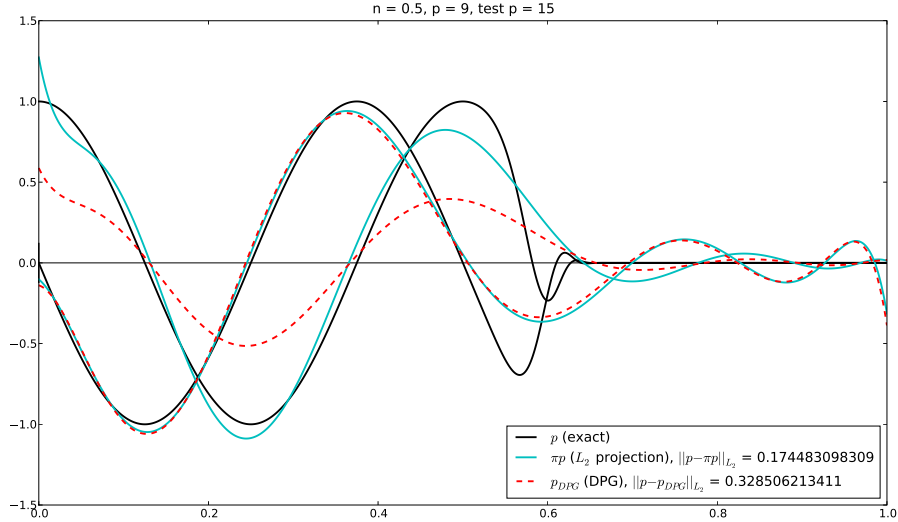
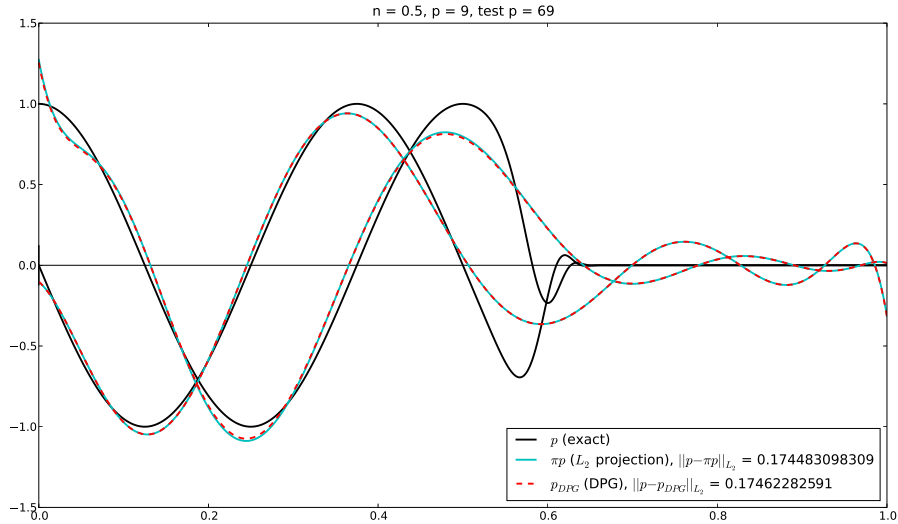
(a) Eight wavelengths, one $p = 4$ element per wavelength(b) 16 wavelengths, 0.5 $p = 8$ elements per wavelength (zoomed)

Figure 13: Higher order approximations

small parameter has been moved to the problem of determining optimal test functions. While the methodology is impractical for, e.g., problems with boundary layers (solving the adjoint equation on a large element is as difficult as solving the original problem), it seems to be perfectly suited for wave propagation where the element size is implied by the need to resolve the wave structure (control of the best approximation error).



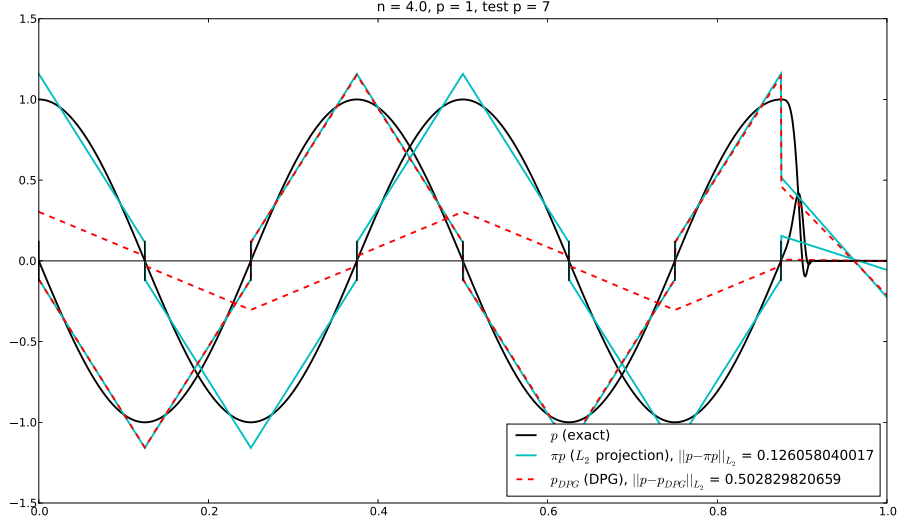
(a) Insufficiently enriched test space



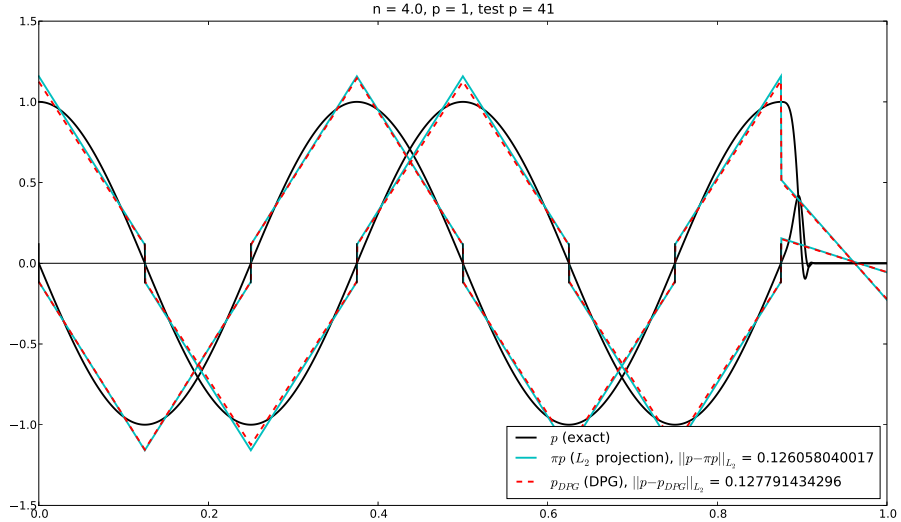
(b) Dramatically enriched test space

Figure 14: Spectral element w/ PML truncation at $x = 0.5$

Performance vs. traditional methods. While extremely stable in contrast to traditional Bubnov-Galerkin approximations for the Helmholtz problem, DPG forces us to consider the mixed problem in which we compute pressure, velocity, and additional fluxes. For a discretization of n elements of order p per wavelength, for a domain of m wavelengths, the DPG formulation requires $2(p+1)mn + 2mn$ degrees of freedom, while a standard H^1 conforming formulation computing only pressure requires pmn . After performing static condensation on the interior degrees of freedom, we are left with a system of dimension $2mn$ for DPG versus mn for the H^1



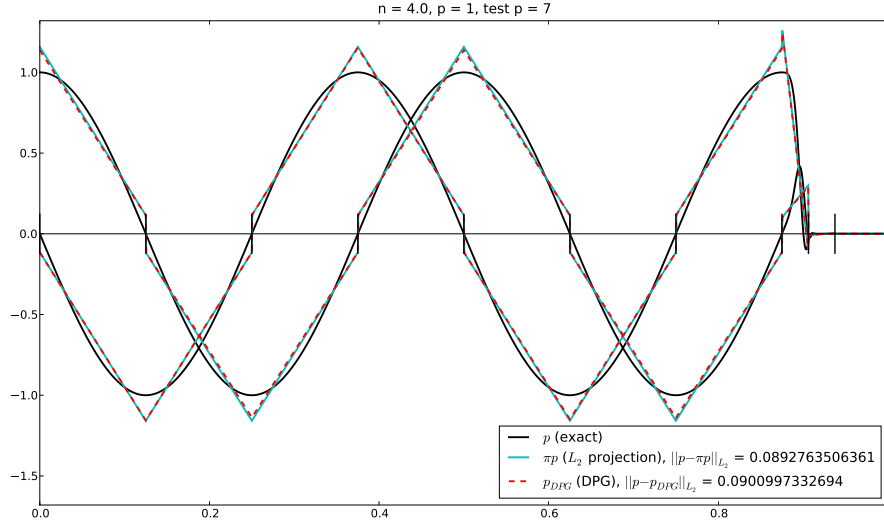
(a) Insufficiently enriched test space



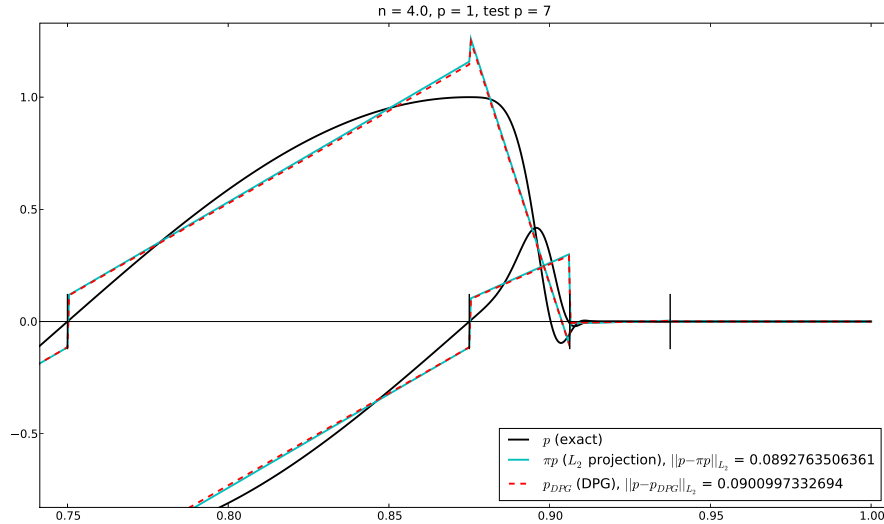
(b) Dramatically enriched test space

Figure 15: Localizable norm; PML occupies one linear element

conforming method. This implies that the DPG method will be competitive when compared with standard finite elements only for large wavenumbers. Here we also remark that while static condensation for the H^1 conforming method requires us to avoid element sizes $h \approx \frac{j\pi}{k}, j \in \mathbb{N}$, in order to avoid the associated interior modes at the given wavenumber, in the mixed formulation



(a)



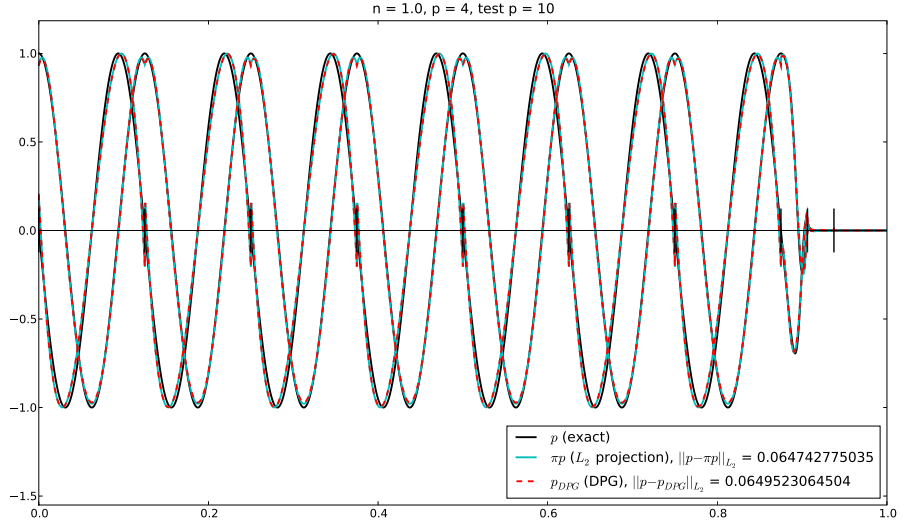
(b) Zoom on PML

Figure 16: Localizable norm, four linear elements per wavelength; refined PML

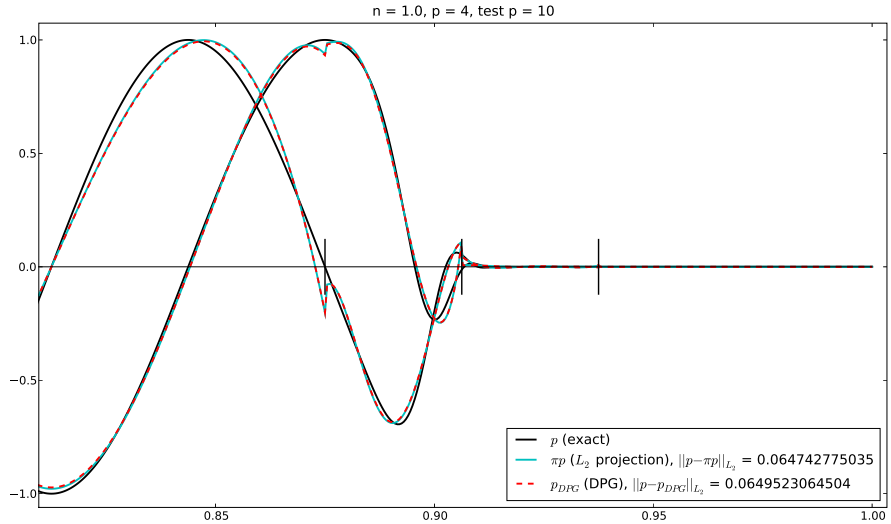
which involves both p and u , there is no such trouble; the problem

$$\begin{aligned} ikp + u' &= 0, \\ iku + p' &= 0, \\ u(x_{i-1}) = u(x_i) = p(x_{i-1}) &= p(x_i) = 0 \end{aligned}$$

admits only the trivial solution.



(a)



(b) Zoom on PML

Figure 17: Localizable norm, one $p = 4$ elements per wavelength; refined PML

Current and future work. The presented analysis and experiments are being extended to 2D problems. Preliminary numerical results indicate that the presented methodology extends to multi-dimensions, with either no, or numerically unobservable, phase error. A 2D version of the method on a structured rectangular mesh does not produce a nine-point stencil, so there is no contradiction with [4]. Our current efforts concentrate on a 2D convergence analysis.

DPG may be an attractive choice for high-frequency wave-propagation problems. The discontinuous formulation offers the possibility of using for trial functions plane waves or other waves

(see, e.g. [14, 21]), with the hope of improving the approximation properties of the underlying space for a given problem. As noted, the element interior submatrices can always be factored without any concern of encountering interior modes, which makes static condensation, nested dissection, and other domain decomposition approaches robust. We emphasize, however, that the control of phase error is related to stability and *not approximability*, and the stability is controlled by the choice of test functions.

APPENDIX A. PROOFS OF THE LEMMAS

Proof of Lemma 3.1. We need to prove that $\|q\|_V^2 = \|ikq + q'\|_{L^2(0,1)}^2 + \frac{1}{2}\|q\|_{L^2(0,1)}^2$ and $\|q\|_V^2 = \|ikq + q'\|_{L^2(0,1)}^2 + |q(1)|^2$ define equivalent norms on $H^1(0,1)$. Let $\tilde{q} = e^{ikx}q$. Since k is real,

$$\|\tilde{q}'\|_{L^2}^2 = \|ikq + q'\|_{L^2}^2, \quad \|\tilde{q}\|_{L^2}^2 = \|q\|_{L^2}^2 \quad \text{and} \quad |\tilde{q}(1)|^2 = |q(1)|^2.$$

Thus, we only need to bound $\|\tilde{q}'\|_{L^2}^2 + |\tilde{q}(1)|^2$ above and below by $\|\tilde{q}'\|_{L^2}^2 + \frac{1}{2}\|\tilde{q}\|_{L^2}^2$.

We use the Fundamental Theorem of Calculus and Young's inequality to estimate $|\tilde{q}(1)|^2$ and $\|\tilde{q}\|_{L^2}^2$. For every $\varepsilon > 0$ and $\delta > 0$,

$$|\tilde{q}(1)|^2 \leq (1 + \varepsilon)\|\tilde{q}\|_{L^2}^2 + \frac{1+\varepsilon}{\varepsilon}\|\tilde{q}'\|_{L^2}^2,$$

$$\|\tilde{q}\|_{L^2}^2 \leq (1 + \delta)|\tilde{q}(1)|^2 + \frac{1+\delta}{\delta}\|\tilde{q}'\|_{L^2}^2.$$

Thus we already see we can obtain the required two sided equivalence with constants independent of k . To obtain the best constants, we first note that the above implies

$$\|q\|_V^2 \leq (1 + \varepsilon^{-1}(1 + \varepsilon))\|\tilde{q}'\|_{L^2}^2 + (1 + \varepsilon)\|\tilde{q}\|_{L^2}^2 \quad (\text{A.44})$$

$$\leq F_1(\varepsilon, \delta)\|\tilde{q}'\|_{L^2}^2 + F_2(\varepsilon, \delta)|\tilde{q}(1)|^2, \quad (\text{A.45})$$

where $F_1(\varepsilon, \delta) = (1 + \frac{1+\varepsilon}{\varepsilon} + (1 + \varepsilon)\frac{1+\delta}{\delta})$ and $F_2(\varepsilon, \delta) = (1 + \varepsilon)(1 + \delta)$. Then we minimize $F_2(\varepsilon, \delta)$ subject to the constraints $\varepsilon > 0, \delta > 0$, and $F_2(\varepsilon, \delta) = F_1(\varepsilon, \delta)$, to obtain $\varepsilon = \frac{\sqrt{2}}{2}$ and $\delta = 1 + \sqrt{2}$. With these values, we have

$$\|q\|_V^2 \leq (2 + \sqrt{2})(\|\tilde{q}'\|_{L^2}^2 + \frac{1}{2}\|\tilde{q}\|_{L^2}^2), \quad \text{by (A.44),}$$

$$(2 + \sqrt{2})(\|\tilde{q}'\|_{L^2}^2 + \frac{1}{2}\|\tilde{q}\|_{L^2}^2) \leq (2 + \sqrt{2})\left(\frac{2 + \sqrt{2}}{2}\right)(\|\tilde{q}'\|_{L^2}^2 + |\tilde{q}(1)|^2), \quad \text{by (A.45).}$$

These two inequalities prove the lemma. \square

Proof of Lemma 3.2. Let us prove that $\check{V}_{hp} \subseteq V_{hp}$. Clearly this will imply that $\check{\rho}_{hp} = \rho_{hp}$ due to unique solvability.

Let $q \in \check{V}_{hp}$ denote the global optimal test function corresponding to $(\rho, \hat{\rho}) \in \check{U}_{hp}$. It solves (3.30), i.e.,

$$\int_0^1 (ikq + q')\overline{(ik\delta q + \delta q')} + \frac{1}{2} \int_0^1 q\overline{\delta q} = \int_0^1 -\rho\overline{(ik\delta q + \delta q')} + \hat{\rho}\overline{\delta q(1)},$$

for all $\delta q \in H^1(0,1)$. As ρ is smooth (a polynomial) within each element K_j , this variational equation translates into the following differential, boundary and interface equations:

$$\begin{cases} -q'' - 2ikq' + (k^2 + \frac{1}{2})q = \rho' + ik\rho & \text{in } (x_{j-1}, x_j) \text{ for } j = 1, \dots, n \\ [ikq + q' + \rho]_j = 0 & \text{for } j = 1, \dots, n-1 \\ (ikq + q' + \rho)(1) = \hat{\rho} \\ -(ikq + q' + \rho)(0) = 0. \end{cases} \quad (\text{A.46})$$

where, as before, the $[\cdot]_j$ denotes the jump of the argument at x_j .

Now, let $\delta q_j \in H^1(K_j)$. Multiplying (A.46)₁ by δq_j , integrating over each element, and summing up over all elements, we get

$$\sum_{j=1}^n \left\{ - \int_{x_{j-1}}^{x_j} (ikq + q' + \rho)' \overline{\delta q_j} - \int_{x_{j-1}}^{x_j} \left(ik(q' + \rho) - (k^2 + \frac{1}{2})q \right) \overline{\delta q_j} \right\} = 0.$$

Integrating the first term by parts, using the continuity of $ikq + q' + \rho$ at element interfaces, and using the boundary conditions in (A.46)_{3,4}, we obtain

$$\begin{aligned} & \sum_{j=1}^n \left\{ (ikq + q', ik\delta q_j + \delta q'_j)_{L^2(K_j)} + \frac{1}{2}(q, \delta q_j)_{L^2(K_j)} \right\} \\ &= \hat{\rho} \overline{\delta q_n}(1) - \sum_{j=1}^n \int_{x_{j-1}}^{x_j} \rho \overline{(ikq_j + q'_j)} + \sum_{j=1}^{n-1} (ikq + q' + \rho)(x_j) [\delta q]_j. \end{aligned}$$

The left hand side equals $(q, \delta q)_{\tilde{V}}$, the inner product in (3.34) for the multielement case. The right hand side is the sesquilinear form of the DPG formulation (3.35) with

$$\begin{aligned} \rho_{hp} &= \hat{\rho}, \\ \hat{\rho}_j^{hp} &= (ikq + q' + p)(x_j), \quad \text{for } j = 1, \dots, n-1, \\ \hat{\rho}_n^{hp} &= \hat{\rho}. \end{aligned}$$

Therefore, the global optimal test function q is a linear combination of the local optimal test functions associated with ρ , $(ikq + q' + p)(x_j)$ and $\hat{\rho}$. \square

Proof of Lemma 4.1. Let $r = \frac{v+q}{2}$ and $s = \frac{v-q}{2}$. Using the same idea as in the proof of Lemma 3.1, we set $\tilde{r} = e^{ikx}r$ and $\tilde{s} = e^{-ikx}s$, so

$$e^{-ikx}\tilde{r}' = ikr + r' \quad \text{and} \quad e^{ikx}\tilde{s}' = -iks + s'.$$

The norm $\|q, v\|_V^2$ can be expressed in terms of these new functions as

$$\left\{ \begin{aligned} \|q, v\|_V^2 &= \|ik(r-s) + (r+s)'\|_{L^2}^2 + \|ik(r+s) + (r-s)'\|_{L^2}^2 + |2r(1)|^2 + |(r+s)(0)|^2 \\ &= \|e^{-ikx}\tilde{r}' + e^{ikx}\tilde{s}'\|_{L^2}^2 + \|e^{-ikx}\tilde{r}' - e^{ikx}\tilde{s}'\|_{L^2}^2 + |2\tilde{r}(1)|^2 + |(\tilde{r} + \tilde{s})(0)|^2 \\ &= 2\|\tilde{r}'\|_{L^2}^2 + 2\|\tilde{s}'\|_{L^2}^2 + |2\tilde{r}(1)|^2 + |(\tilde{r} + \tilde{s})(0)|^2. \end{aligned} \right.$$

On one hand we have

$$\begin{aligned} |2\tilde{r}(1)|^2 &\leq (1 + \varepsilon_1) \|2\tilde{r}\|_{L^2}^2 + 4 \left(\frac{1+\varepsilon_1}{\varepsilon_1} \right) \|\tilde{r}'\|_{L^2}^2 \\ |(\tilde{r} + \tilde{s})(0)|^2 &\leq (1 + \varepsilon_2) \|\tilde{r} + \tilde{s}\|_{L^2}^2 + \frac{1+\varepsilon_2}{\varepsilon_2} \|\tilde{r}' + \tilde{s}'\|_{L^2}^2 \\ &\leq (1 + \varepsilon_2) \|\tilde{r} + \tilde{s}\|_{L^2}^2 + \frac{1+\varepsilon_2}{\varepsilon_2} \left((1 + \varepsilon_3) \|\tilde{r}'\|_{L^2}^2 + \frac{1+\varepsilon_3}{\varepsilon_3} \|\tilde{s}'\|_{L^2}^2 \right). \end{aligned}$$

Observe that $\|2\tilde{r}\|_{L^2}^2 = \|v + q\|_{L^2}^2$ and $\|\tilde{r} + \tilde{s}\|_{L^2}^2 = \|v \cos(kx) + iq \sin(kx)\|_{L^2}^2$.

On the other hand, we have

$$\begin{aligned} \|2\tilde{r}\|_{L^2}^2 &\leq (1 + \delta_1)|2\tilde{r}(1)|^2 + 4\left(\frac{1+\delta_1}{\delta_1}\right)\|\tilde{r}'\|_{L^2}^2 \\ \|\tilde{r} + \tilde{s}\|_{L^2}^2 &\leq (1 + \delta_2)|(\tilde{r} + \tilde{s})(0)|^2 + \frac{1+\delta_2}{\varepsilon_2}\|\tilde{r}' + \tilde{s}'\|_{L^2}^2 \\ &\leq (1 + \delta_2)|(\tilde{r} + \tilde{s})(0)|^2 + \frac{1+\delta_2}{\delta_2}\left((1 + \delta_3)\|\tilde{r}'\|_{L^2}^2 + \frac{1+\delta_3}{\varepsilon_3}\|\tilde{s}'\|_{L^2}^2\right). \end{aligned}$$

We choose $\varepsilon_1 = \varepsilon_2$, $\delta_1 = \delta_2$ and $\varepsilon_3 = \delta_3 = \sqrt{5} - 2$. In consequence,

$$\left\{ \begin{array}{l} \|q, v\|_V^2 \leq (1 + f_1(\varepsilon_1))\left(2\|\tilde{r}'\|_{L^2}^2 + 2\|\tilde{s}'\|_{L^2}^2\right) + f_2(\varepsilon_1)\left(\|2\tilde{r}\|_{L^2}^2 + \|\tilde{r} + \tilde{s}\|_{L^2}^2\right) \\ \leq (1 + f_1(\varepsilon_1) + f_2(\varepsilon_1)f_1(\delta_1))\left(2\|\tilde{r}'\|_{L^2}^2 + 2\|\tilde{s}'\|_{L^2}^2\right) \\ + f_2(\varepsilon_1)f_2(\delta_1)\left(|2\tilde{r}(1)|^2 + |(\tilde{r} + \tilde{s})(0)|^2\right), \end{array} \right. \quad (\text{A.47})$$

where the functions of f_1 and f_2 are defined by :

$$f_1(x) = C\left(\frac{1+x}{x}\right), \quad f_2(x) = (1+x) \quad \text{and} \quad C = \frac{\sqrt{5}+3}{2}.$$

We arrive at the minimization problem :

$$\left\{ \begin{array}{l} \min f_2(\varepsilon_1)f_2(\delta_1) \\ \varepsilon_1 > 0 \\ \delta_1 > 0 \\ 1 + f_1(\varepsilon_1) + f_2(\varepsilon_1)f_1(\delta_1) - f_2(\varepsilon_1)f_2(\delta_1) = 0, \end{array} \right.$$

whose solutions are $\varepsilon_1 = \sqrt{\frac{C}{C+1}}$ and $\delta_1 = f_1(\varepsilon_1)$. Replacing these values on the inequality (A.47) we obtain :

$$\left\{ \begin{array}{l} \|q, v\|_V^2 \leq \sqrt{C+1}(\sqrt{C} + \sqrt{C+1})\left(2\|\tilde{r}'\|_{L^2}^2 + 2\|\tilde{s}'\|_{L^2}^2 + \frac{1}{C+1}(\|2\tilde{r}\|_{L^2}^2 + \|\tilde{r} + \tilde{s}\|_{L^2}^2)\right) \\ \leq \sqrt{C+1}(\sqrt{C} + \sqrt{C+1})\left(1 + \sqrt{\frac{C}{C+1}}\right)\|q, v\|_V^2. \end{array} \right.$$

Hence,

$$C_1 = \left(1 + \sqrt{\frac{C}{C+1}}\right)^{-1} = \sqrt{C+1}(\sqrt{C+1} - \sqrt{C}) = \frac{5+\sqrt{5}}{2} - (5 + 2\sqrt{5})^{\frac{1}{2}},$$

$$C_2 = \sqrt{C+1}(\sqrt{C+1} + \sqrt{C}) = \frac{5+\sqrt{5}}{2} + (5 + 2\sqrt{5})^{\frac{1}{2}}.$$

□

REFERENCES

- [1] M. Ainsworth and H. Wajid. Optimally blended spectral-finite element scheme for wave propagation, and non-standard reduced integration. *University of Strathclyde Mathematics Research Report*, 12, 2009.
- [2] I. Babuška, F. Ihlenburg, E.T. Paik, and S.A. Sauter. A generalized finite element method for solving the Helmholtz equation in two dimensions with minimal pollution. *Comput. Methods Appl. Mech. Engrg.*, 128:325–359, 1995.
- [3] I. Babuska and J. M. Melenk. The partition of unity method. *International Journal of Numerical Methods in Engineering*, 40:727–758, 1996.
- [4] Ivo M. Babuska and Stefan A. Sauter. Is the pollution effect of the fem avoidable for the helmholtz equation considering high wave numbers? *SIAM J. Numer. Anal.*, 34(6):2392–2423, 1997.

- [5] P. E. Barbone and I. Harari. Nearly H^1 -optimal finite element methods. *Comput. Methods Appl. Mech. Engrg.*, 190:5679 – 5690, 2001.
- [6] Z. Cai, R. Lazarov, T. A. Manteuffel, and S. F. McCormick. First-order system least squares for second-order partial differential equations. *SIAM J. Numer. Anal.*, 31:1785 – 1799, 1994.
- [7] R. Courant and K. O. Friedrichs. *Supersonic Flow and Shock Waves*. Interscience Publishers, Inc., New York, N.Y., 1948.
- [8] L. Demkowicz. Babuška \Leftrightarrow Brezzi ? Technical report, ICES, 2006.
- [9] L. Demkowicz and J. Gopalakrishnan. A class of discontinuous Petrov-Galerkin methods. Part I: The transport equation. *Comput. Methods Appl. Mech. Engrg.*, 2009. accepted, see also ICES Report 2009-12.
- [10] L. Demkowicz and J. Gopalakrishnan. A class of discontinuous Petrov-Galerkin methods. Part II: Optimal test functions. Technical Report 16, ICES, 2009. Numer. Meth. Part. D. E., in review.
- [11] L. Demkowicz, J. Gopalakrishnan, and A. Niemi. A class of discontinuous Petrov-Galerkin methods. Part III: Adaptivity. Technical Report 1, ICES, 2010.
- [12] L. Demkowicz and J. T. Oden. An adaptive characteristic Petrov-Galerkin finite element method for convection-dominated linear and nonlinear parabolic problems in one space variable. *Journal of Computational Physics*, 68(1):188–273, 1986.
- [13] L. Demkowicz and J. T. Oden. An adaptive characteristic Petrov-Galerkin finite element method for convection-dominated linear and nonlinear parabolic problems in two space variables. *Comput. Methods Appl. Mech. Engrg.*, 55(1-2):65–87, 1986.
- [14] C. Farhat, I. Harari, and L. P. Franca. The discontinuous enrichment method. *Computer Methods in Applied Mechanics and Engineering*, 190(48):6455 – 6479, 2001.
- [15] Charbel Farhat, Isaac Harari, and Ulrich Hetmaniuk. A discontinuous galerkin method with lagrange multipliers for the solution of helmholtz problems in the mid-frequency regime. *Computer Methods in Applied Mechanics and Engineering*, 192(11-12):1389 – 1419, 2003.
- [16] X. Feng and H. Wu. Discontinuous Galerkin methods for the Helmholtz equation with large wave number. *SIAM J. Numer. Anal.*, 47:2872 – 2896, 2009.
- [17] Leopoldo P. Franca, Charbel Farhat, Antonini P. Macedo, and Michel Lesoinne. Residual-free bubbles for the helmholtz equation. Technical report, Denver, CO, USA, 1996.
- [18] Dan Givoli. Nonlocal and semilocal optimal weighting functions for symmetric problems involving a small parameter. *Internat. J. Numer. Methods Engrg.*, 26(6):1281–1298, 1988.
- [19] Isaac Harari. A survey of finite element methods for time-harmonic acoustics. *Computer Methods in Applied Mechanics and Engineering*, 195(13-16):1594 – 1607, 2006. A Tribute to Thomas J.R. Hughes on the Occasion of his 60th Birthday.
- [20] Isaac Harari and Thomas J. R. Hughes. Finite element methods for the helmholtz equation in an exterior domain: Model problems. *Computer Methods in Applied Mechanics and Engineering*, 87(1):59 – 96, 1991.
- [21] R. Hiptmair, A. Moiola, and I. Perugia. Plane wave discontinuous Galerkin methods for the 2D Helmholtz equation: analysis of the p -version. Technical Report 20, Seminar for Applied Mathematics, ETH Zurich, 2009.
- [22] T.J.R. Hughes and A. Brooks. A multidimensional upwind scheme with no crosswind diffusion. In *Finite Element Methods for Convection Dominated Flows (Papers, Winter Ann. Meeting Amer. Soc. Mech. Engrs., New York, 1979)*, volume 34 of *AMD*, pages 19–35, New York, 1979. Amer. Soc. Mech. Engrs. (ASME).
- [23] F. Ihlenburg. *Finite Element Analysis of Acoustic Scattering*, volume 132 of *Applied Mathematical Sciences*. Springer-Verlag, New York, 1998.
- [24] A. F. D. Loula and D. T. Fernandes. A quasi optimal Petrov-Galerkin method for Helmholtz problem. *Internat. J. Numer. Methods Engrg.*, 80:1595 – 1622, 2009.
- [25] Assad A. Oberai and Peter M. Pinsky. A numerical comparison of finite element methods for the Helmholtz equation. *Journal of Computational Acoustics*, 8(1):211, 2000.
- [26] J.T. Oden and L.F. Demkowicz. *Applied Functional Analysis for Science and Engineering*. Chapman & Hall/CRC Press, Boca Raton, 2010. Second edition.
- [27] Lonny L. Thompson. A review of finite-element methods for time-harmonic acoustics. *The Journal of the Acoustical Society of America*, 119(3):1315–1330, 2006.
- [28] Lonny L. Thompson and Peter M. Pinsky. A Galerkin least squares finite element method for the two-dimensional Helmholtz equation. *International Journal for Numerical Methods in Engineering*, 38:371 – 397, 1995.
- [29] K. Yosida. *Functional Analysis*. Springer-Verlag, Berlin, 1995. Reprint of the sixth (1980) edition.

INSTITUTE FOR COMPUTATIONAL ENGINEERING AND SCIENCES, THE UNIVERSITY OF TEXAS AT AUSTIN,
AUSTIN, TX 78712, USA

E-mail address: jzitelli@ices.utexas.edu

INSTITUTO DE MATEMÁTICAS, PONTIFICIA UNIVERSIDAD CATÓLICA DE VALPARAÍSO, CHILE AND INSTITUTE
FOR COMPUTATIONAL ENGINEERING AND SCIENCES, THE UNIVERSITY OF TEXAS AT AUSTIN, AUSTIN, TX 78712,
USA

E-mail address: muga@ices.utexas.edu

INSTITUTE FOR COMPUTATIONAL ENGINEERING AND SCIENCES, THE UNIVERSITY OF TEXAS AT AUSTIN,
AUSTIN, TX 78712, USA

E-mail address: leszek@ices.utexas.edu

DEPARTMENT OF MATHEMATICS, UNIVERSITY OF FLORIDA, GAINESVILLE, FL 32611–8105, USA

E-mail address: jayg@ufl.edu

IKERBASQUE AND BCAM, BILBAO, SPAIN

E-mail address: pardo@bcamath.org

APPLIED MATHEMATICS AND COMPUTATIONAL SCIENCE, EARTH AND SCIENCE ENGINEERING, KING ABDUL-
LAH UNIVERSITY OF SCIENCE AND TECHNOLOGY (KAUST), SAUDI ARABIA

E-mail address: victor.calo@kaust.edu.sa